AD-A034 276 AIR FORCE INST OF TECH WRIGHT-PATTERSON AFB OHIO SCH--ETC F/G 20/3
ELECTROMAGNETIC SCATTERING BY CONCENTRIC FINITE CYLINDERS.(U)
DEC 76 D G ARDIS
UNCLASSIFIED GE/EE/76-13 NL

| OF |
AD
A034276

END
DATE
FILMED
2-77

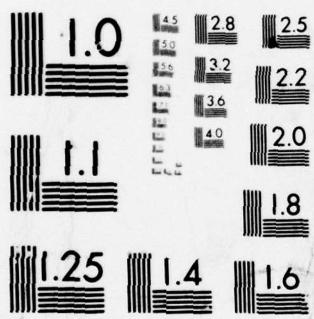

MICROCOPY RESOLUTION TEST CHART
NATIONAL BUREAU OF STANDARDS-1963-A

GE/EE/76-13

1

ELECTROMAGNETIC SCATTERING BY CONCENTRIC FINITE CYLINDERS

THESIS

GE/EE/76-13

David G. Ardis
Captain USAF

(See form 1473)

GE/EE/76-13

ELECTROMAGNETIC SCATTERING BY CONCENTRIC FINITE CYLINDERS

THESIS

Presented to the Faculty of the School of Engineering
of the Air Force Institute of Technology
Air University
in Partial Fulfillment of the
Requirements for the Degree of
Master of Science

by

David G. Ardis, B.S.
Captain USAF
Graduate Electrical Engineering
December 1976

Preface

This thesis was originally conceived as a study of scattering by circular cylinders with end caps, apertures, and internal cavities with a wire passing through the cavities. After some research and discussion with scholars knowledgeable in this area of study, it was decided to accept the suggestions of Dr. Chalmers M. Butler and limit the analysis to scattering by two concentric finite circular cylinders.

I am deeply grateful to my thesis advisor Dr. William A. Davis who made the degree of success that was attained possible by spending many hours explaining the concepts involved and how to apply them. Finally, I owe special thanks to my family who have sacrificed tremendously that I might complete this work and in particular to my wife Mary Jo for typing and editing this manuscript.

Contents

List of Figures

Abstract

This thesis deals with electromagnetic scattering from two concentric finite length cylinders. The scattering bodies are assumed to be perfect electric conductors and the incident field is assumed to be a plane wave whose magnetic field is transverse to the longitudinal axis of the scatterers. Electromagnetic field equations are derived in terms of vector potentials. Integral equations are developed for the surface currents induced on the cylinders. A numerical solution is formulated in terms of the method of moments for the unknown surface currents and the components of the scattered electric field. Results are presented for scatterers of different dimensions. Comparisons are made between scattering from a finite hollow cylinder and scattering from two concentric finite cylinders.

I. Introduction

Survivability in a nuclear war environment is a facet of weapon system design that must be considered if the weapon system is to be effective in such an environment. In addition to other effects, one must consider the effect of the electromagnetic pulse (EMP) generated by a nuclear detonation. EMP may induce large currents in a weapon system which damage or destroy critical electronic components, possibly rendering the system ineffective. Thus, one needs to be able to predict these currents and design the system to minimize their effects. There are three approaches that could be used to obtain EMP data. One could detonate a nuclear device and measure the induced currents. This is obviously impractical for environmental and political considerations. Secondly, one could build a simulator which produces electronically a wave similar to an EMP. The Air Force Weapons Laboratory has an EMP simulator which is used to obtain test data. Unfortunately, it is impractical to test all systems in this manner. The final approach to predicting EMP effects is to formulate the problem as an electromagnetic scattering problem.

The electromagnetic scattering approach is pleasing in that one could determine the EMP effects on different designs without actually building the different systems and, theoretically, any system could be evaluated. However, the number of structures for which the scattering problem can be solved analytically is severely limited. In general, analytic solutions are limited to small classes of canonical structures. The advent of the high speed digital computer has permitted the analysis of electromagnetic scattering by more general structures through numerical approximation methods. Although much work has been devoted to this approach, many more structures need to be simulated before an accurate prediction can be made of the EMP currents induced on complex structures such as aircraft or missles.

This thesis represents an effort to analyze the electromagnetic scattering from two concentric finite-length cylinders. Davis (Ref 4) investigated electromagnetic scattering by a finite hollow cylinder. The problem considered here will be restricted in a manner similar to Davis's by considering only perfect electric conductors and transverse magnetic plane wave incidence. An effort is made to present the differences between scattering from a finite hollow cylinder and the scattering from the same cylinder with an inner cylinder, or wire, whose radius is much smaller than the radius of the outer cylinder.

The information in this thesis is grouped into chapters based on the traditional subdivisions and the theoretical and mathematical concepts that must be considered in solving this type of problem. Chapter II contains the theoretical development. Electric and magnetic field equations are developed in terms of vector potentials instead of the electromagnetic field quantities themselves. This permits one to assume a lower degree of smoothness on electromagnetic fields while maintaining a rigorous development. The field equations are then manipulated to give integral equations for the equivalent currents induced on a scattering surface by an incident field. The electric field integral equation is finally specialized to scattering by both the concentric cylinders and the hollow cylinder.

Chapter III describes how one might solve the equations developed in Chapter II on a digital computer. The method of moments is described briefly and then applied to the scattering current equations. This results in a system of simultaneous linear algebraic equations whose solution represents an approximation of the induced currents. Some manipulations are shown which facilitate solving this system of equations on a digital computer. Finally, digitized expressions for the total electric field are developed.

Chapter IV presents plots which illustrate the validity of the results and the differences between the scattering from a hollow cylinder and the scattering from the concentric cylinders. Comparisons are made between Harrington's solution for scattering from an infinite cylinder (Ref 7) and scattering from finite cylindrical structures. Plots are included for cylinders whose dimensions simulate structures of interest to the Air Force.

Chapter V presents conclusions that can be drawn about scattering from concentric cylinders relative to scattering from hollow cylinders. Finally, recommendations are made for a series of problems which would extend this work and provide data that would be useful in the design of weapon systems.

Three references were particularly useful in the development of thi thesis. The dissertation by Davis (Ref 4) and Harrington's book (Ref 7) on electromagnetic field theory were used extensively in the theoretical development. Harrington's book (Ref 6) on the method of moments was used for analysis of how to digitize the theoretical equations for computer implementation. Finally, the series of reports published by the Air Force Weapons Laboratory as Electromagnetic Pulse Interaction Notes were used to gain insight into the magnitude of the EMP problem and the geometries that have been investigated previously.

II. Theoretical Development

Integral expressions for the electric $\bar{E}$ and magnetic $\bar{H}$ fields that exist in an electromagnetic scattering problem can be derived in terms of a magnetic vector potential $\bar{A}$ and an electric vector potential $\bar{F}$ (Ref 7:77). In general, fields can be expressed as

$$\bar{C} = \bar{C}^i + \bar{C}^s \tag{1}$$

where $\bar{C}$ represents the total field, $\bar{C}^i$ represents the incident field or the field that would be present if there were no scatterer, and $\bar{C}^s$ represents the field due to the scatterer. The scattered fields in electromagnetic scattering problems are due to equivalent electric and magnetic currents induced on the scattering body by the incident field. When appropriate boundary conditions are imposed, determining the total electromagnetic fields reduces to solving an integral equation for the unknown equivalent currents on the scattering body. In this chapter, vector potentials and Maxwell's equations are used to develop integral equations for the equivalent currents on a finite hollow cylinder and the equivalent currents on a finite cylinder and wire, the bodies being perfect electric conductors and the wire being on the longitudinal axis of the cylinder.

Vector Potential Equations

The bases of all electromagnetic field problems are

Maxwell's equations. For simple matter, that is, matter that is homogenous, linear, isotropic, and time invariant, Maxwell's equations can be written in differential form ($e^{j\omega t}$ time variation suppressed) as

$$\nabla \times \bar{H} = j\omega\varepsilon\bar{E} + \bar{J} \tag{2}$$

$$\nabla \times \bar{E} = -j\omega\mu\bar{H} - \bar{M} \tag{3}$$

$$\nabla \cdot \bar{E} = \rho_e/\varepsilon \tag{4}$$

$$\nabla \cdot \bar{H} = m/\mu \tag{5}$$

where $\bar{E}$ and $\bar{H}$ are electric and magnetic field intensities, $\bar{J}$ and $\bar{M}$ are electric and magnetic current densities, and ρ_e and m are the electric and magnetic charge densities. Taking the divergence of Eqs (2) and (3), substituting into Eqs (4) and (5), and noting that the divergence of a curl is zero, yields the continuity equations

$$\nabla \cdot \bar{J} = -j\omega\rho_e \tag{6}$$

$$\nabla \cdot \bar{M} = -j\omega m \tag{7}$$

An expression for the electromagnetic fields in terms of the magnetic vector potential $\bar{A}$ can be derived by assuming there are no magnetic current sources, $\bar{M} = 0$, and taking the divergence of Eq (3). This yields $\nabla \cdot \bar{H} = 0$. Pierce (Ref 10:221) states that for any vector whose divergence is identically zero everywhere, there exists a vector whose curl equals the original vector. Therefore, let

$$\bar{H} = \nabla \times \bar{A} \tag{8}$$

where $\bar{A}$ is defined as a magnetic vector potential. Substituting for $\bar{H}$ in Eq (3) yields

$$\nabla \times (\bar{E} + j\omega\mu\bar{A}) = 0 \tag{9}$$

For any vector whose curl is identically zero everywhere, there exists a scalar whose gradient equals the vector (Ref 10:221). Therefore, let

$$\bar{E} + j\omega\mu\bar{A} = -V \tag{10}$$

where V is defined as an electric scalar potential. Substituting for $\bar{E}$ in Eq (2) yields

$$\nabla \times \nabla \times \bar{A} = j\omega\varepsilon(-j\omega\mu\bar{A} - \nabla V) + \bar{J} \tag{11}$$

Helmholtz (Ref 10:221) showed that a vector is completely specified to within a constant when both its curl and divergence are given. To complete the specifications of $\bar{A}$, let the divergence of $\bar{A}$ be

$$\nabla \cdot \bar{A} = -j\omega\varepsilon V \tag{12}$$

Substituting Eq (12) into Eq (11) and using the vector identity

$$\nabla \times \nabla \times \bar{A} = \nabla(\nabla \cdot \bar{A}) - \nabla^2\bar{A} \tag{13}$$

results in

$$\nabla^2\bar{A} + k^2\bar{A} = -\bar{J} \tag{14}$$

where k $=\omega^2\mu\varepsilon$. Substituting Eqs (8) and (14) into Eq (2) yields

$$j\omega\varepsilon\bar{E} = k^2\bar{A} + \nabla(\nabla\cdot\bar{A}) \tag{15}$$

If there are only magnetic current sources, $\bar{J} = 0$, one can write by the principle of duality (Ref 7:99)

$$\nabla^2\bar{F} + k^2\bar{F} = -\bar{M} \tag{16}$$

and

$$\bar{E} = -\nabla\times\bar{F} \tag{17}$$

$$j\omega\mu\bar{H} = k^2\bar{F} + \nabla(\nabla\cdot\bar{F}) \tag{18}$$

where $\bar{F}$ is defined as an electric vector potential. If both electric and magnetic current sources are present, one can write by the principle of superposition

$$\bar{E} = \frac{1}{j\omega\varepsilon}\left[k^2\bar{A} + \nabla(\nabla\cdot\bar{A})\right] - \nabla\times\bar{F} \tag{19}$$

$$\bar{H} = \frac{1}{j\omega\mu}\left[k^2\bar{F} + \nabla(\nabla\cdot\bar{F})\right] + \nabla\times\bar{A} \tag{20}$$

Thus, once $\bar{A}$ and $\bar{F}$ are known, the electromagnetic fields $\bar{E}$ and $\bar{H}$ can be determined.

Scattering Equations

Equations (19) and (20) represent the total electric and magnetic fields in simple matter obtained from independent vector potentials. If a scattering body is placed in the medium, the solution for the fields becomes somewhat more complicated since the vector potentials are composed of incident and scattered components. One must calculate the scattered vector potentials prior to solving for the electromagnetic fields.

The vector potentials $\bar{A}$ and $\bar{F}$ due to finite independent sources in simple matter, enclosed in a volume V, at any point $\bar{r}$ in all space are (Ref 7:100)

$$\bar{A}(\bar{r}) = \int_V \bar{J}\, \Phi(\bar{r}, \bar{r}')\, dv' \tag{21}$$

$$\bar{F}(\bar{r}) = \int_V \bar{M}\, \Phi(\bar{r}, \bar{r}')\, dv' \tag{22}$$

where the prime notation indicates "with respect to the source coordinates". Note that use has been made of the three dimensional free space Green's function

$$\Phi(\bar{r}, \bar{r}') = \frac{e^{-jk|\bar{r}-\bar{r}'|}}{4\pi|\bar{r}-\bar{r}'|} \tag{23}$$

The scattered components of the vector potentials for a scattering body can also be shown to be given by the forms Eqs (21) and (22). This may be shown by considering the scattering body in simple matter as depicted in Figure 1. All independent sources $\bar{J}$ are in volume V which is bounded by the surface of the scatterer S and the surface S_1 which approaches infinity. The unit normal vector $\hat{n}$ at S points into V.

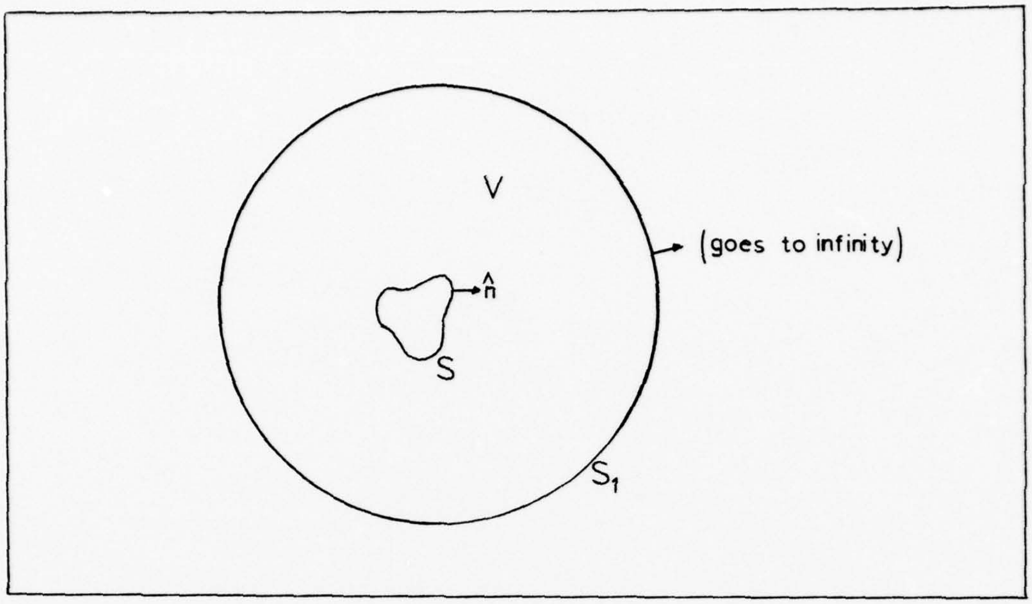

Figure 1. Scattering Geometry

To determine the scattered field components, consider the identity (Ref 11:300)

$$\iint_V \left\{ \Phi \nabla \times \nabla \times \bar{A}(\bar{r}) + \bar{A}(\bar{r}) \nabla^2 \Phi + \nabla \Phi \left[\nabla \cdot \bar{A}(\bar{r}) \right] \right\} dv =$$

$$- \oint_{\partial V} \left\{ - \nabla \Phi \times \left[\hat{n} \times \bar{A}(\bar{r}) \right] + \left[\hat{n} \cdot \bar{A}(\bar{r}) \right] \nabla \Phi + \hat{n} \Phi \times \left[\nabla \times \bar{A}(\bar{r}) \right] \right\} ds \tag{24}$$

where the observation point $\bar{r}$ is not on the closed regular surface ∂V, the boundary on V formed by S and S_1. It is assumed that the field $\bar{A}$ meets the Sommerfeld radiation conditions (Ref 2:20), is continuous with a continuous first derivative on S, and has a continuous second derivative in V in the sense of distributions (Ref 1:114). Hence, the surface integral over S_1 is zero and Eq (24) may be written as

$$\int_V \left\{ \Phi \nabla\times\nabla\times \bar{A}(\bar{r}) + \bar{A}(\bar{r})\nabla^2\Phi + \nabla\Phi\left[\nabla\cdot\bar{A}(\bar{r})\right]\right\} dv =$$

$$-\oint_S \left\{ -\nabla\Phi\times\left[\hat{n}\times\bar{A}(\bar{r})\right] + \left[\hat{n}\cdot\bar{A}(\bar{r})\right]\nabla\Phi + \hat{n}\Phi\times\left[\nabla\times\bar{A}(\bar{r})\right]\right\} ds \qquad (25)$$

Using Eq (14) and the expression (Ref 8:340)

$$\nabla^2\Phi + k^2\Phi = -\delta(\bar{r}-\bar{r}') \qquad (26)$$

where $\delta(\bar{r} - \bar{r}')$ is the Dirac Delta Function, a generalized function or distribution as described by Wylie (Ref 12:317), one can write

$$\bar{A}(\bar{r}) = \int_V \Phi\, \bar{J}\, dv + \oint_S \left\{ \Phi\, \hat{n}'\times\left[\nabla'\times\bar{A}(\bar{r}')\right] + \left[\hat{n}'\cdot\bar{A}(\bar{r}')\right]\nabla'\Phi \right.$$

$$\left. - \hat{n}'\Phi\left[\nabla'\cdot\bar{A}(\bar{r}')\right] - \nabla'\Phi\times\left[\hat{n}'\times\bar{A}(\bar{r}')\right]\right\} ds' \qquad (27)$$

where the reference system has been changed by interchanging the prime and unprime notation.

One needs $\nabla[\nabla\cdot\bar{A}(\bar{r})]$ and $\nabla\times\bar{A}(\bar{r})$ to determine $\bar{E}(\bar{r})$ and $\bar{H}(\bar{r})$. The identities (see Appendix)

$$\nabla\times\oint_S \nabla'\Phi\times\left[\hat{n}'\times\bar{A}(\bar{r}')\right] ds' = -\oint_S \Phi\, \hat{n}'\times k^2\bar{A}(\bar{r}')\, ds'$$

$$- \nabla\left[\nabla\cdot\oint_S \Phi\, \hat{n}'\times\bar{A}(\bar{r}')\, ds'\right] \qquad (28)$$

and

$$\nabla\left\{\nabla\cdot\oint_S \hat{n}'\Phi\times\left[\nabla'\cdot\bar{A}(\bar{r}')\right] ds'\right\} = 0 \qquad (29)$$

can be used to show that

$$\nabla[\nabla\cdot\bar{A}(\bar{r})] = \nabla\left[\nabla\cdot\int_V \Phi\, \bar{J}\, dv'\right] + \oint_S \left\{\left[\hat{n}'\times(\nabla\times\bar{A}(\bar{r}'))\cdot\nabla'\right]\nabla'\Phi\right.$$

$$\left. - k^2\nabla'\Phi\left[\hat{n}'\cdot\bar{A}(\bar{r}')\right] - \left[\nabla'\cdot\bar{A}(\bar{r}')\right](\hat{n}'\cdot\nabla')\nabla'\Phi\right\} ds' \qquad (30)$$

and $$\nabla\times\bar{A}(\bar{r}) = \nabla\times\int_V \Phi\,\bar{J}\,dv' + \nabla\times\oint_S \Phi\,\hat{n}'\times\left[\nabla'\times\bar{A}(\bar{r}')\right]ds'$$

$$-\frac{k^2}{j\omega\mu}\oint_S \frac{1}{j\omega\varepsilon}\Phi\,\hat{n}'\times\left\{\nabla'\left[\nabla'\cdot\bar{A}(\bar{r}')\right]+k^2\bar{A}(\bar{r}')\right\}ds'$$

$$-\frac{1}{j\omega\mu}\nabla\left\{\nabla\cdot\oint_S \frac{1}{j\omega\varepsilon}\Phi\,\hat{n}'\times\left[\nabla'(\nabla'\cdot\bar{A}(\bar{r}'))+k^2\bar{A}(\bar{r}')\right]ds'\right\} \qquad (31)$$

Thus, the expression for the total electric field is

$$j\omega\varepsilon\bar{E}(\bar{r}) = k^2\int_V \Phi\,\bar{J}\,dv' + \nabla\left(\nabla\cdot\int_V \Phi\,\bar{J}\,dv'\right)$$

$$+k^2\oint_S\Big\{\Phi\,\hat{n}'\times\left[\nabla'\times\bar{A}(\bar{r}')\right] - \hat{n}'\Phi\left[\nabla'\cdot\bar{A}(\bar{r}')\right]$$

$$-\nabla'\Phi\times\left[\hat{n}'\times\bar{A}(\bar{r}')\right]\Big\}ds' + \oint_S\left\{\hat{n}'\times\left[\nabla'\times\bar{A}(\bar{r}')\right]\cdot\nabla'\right\}\nabla'\Phi\,ds'$$

$$-\oint_S\left[\nabla'\cdot\bar{A}(\bar{r}')\right](\hat{n}'\cdot\nabla')\nabla'\Phi\,ds' \qquad (32)$$

which may be rewritten as

$$j\omega\varepsilon\,\bar{E}(\bar{r}) = k^2\bar{A}^i(\bar{r}) + \nabla\left[\nabla\cdot\bar{A}^i(\bar{r})\right] + k^2\oint_S \Phi\,\hat{n}'\times\left[\nabla'\times\bar{A}(\bar{r}')\right]ds'$$

$$+\nabla\times\oint_S \Phi\,\hat{n}'\times\nabla'\left[\nabla'\cdot\bar{A}(\bar{r}')\right]ds' + \oint_S\left\{\hat{n}'\times\left[\nabla'\times\bar{A}(\bar{r}')\right]\cdot\nabla'\right\}\nabla'\Phi\,ds'$$

$$+\nabla\times\oint_S k^2\Phi\,\hat{n}'\times\bar{A}(\bar{r}')\,ds' \qquad (33)$$

where $\bar{A}^i(\bar{r})$ is the magnetic vector potential due to the independent source $\bar{J}$ and $\bar{A}(\bar{r}')$ is the total magnetic vector potential at S. The preceding equation may be written in simpler form by using the unit dyadic $\bar{\bar{I}}$ (Ref 9:569)

$$j\omega\epsilon\,\bar{E}(\bar{r}) = \left[k^2\bar{\bar{I}} + \nabla\nabla\right]\cdot \bar{A}^i(\bar{r}) + \nabla\times\oint_S \Phi\,\hat{n}'\times\left[k^2\bar{\bar{I}}\right.$$

$$\left. + \nabla'\nabla'\right]\cdot \bar{A}(\bar{r}')\,ds' + \left[k^2\bar{\bar{I}} + \nabla\nabla\right]\cdot\oint_S \Phi\,\hat{n}'\times\left[\nabla'\times\bar{A}(\bar{r}')\right]ds' \qquad (34)$$

Using the same notation, one may write the magnetic field equation as

$$\bar{H}(\bar{r}) = \nabla\times\bar{A}^i(\bar{r}) + \nabla\times\oint_S \Phi\,\hat{n}'\times\left[\nabla'\times\bar{A}(\bar{r}')\right]ds'$$

$$+ \left[k^2\bar{\bar{I}} + \nabla\nabla\right]\cdot\oint_S \frac{1}{k^2}\Phi\,\hat{n}'\times\left[k^2\bar{\bar{I}} + \nabla'\nabla'\right]\cdot\bar{A}(\bar{r}')\,ds' \qquad (35)$$

If the only independent source is a magnetic current source, then by duality $\bar{E}(\bar{r})$ and $\bar{H}(\bar{r})$ are

$$\bar{E}(\bar{r}) = -\nabla\times\bar{F}^i(\bar{r}) - \nabla\times\oint_S \Phi\,\hat{n}'\times\left[\nabla'\times\bar{F}(\bar{r}')\right]ds'$$

$$+ \left[k^2\bar{\bar{I}} + \nabla\nabla\right]\cdot\oint_S \frac{1}{k^2}\Phi\,\hat{n}'\times\left[k^2\bar{\bar{I}} + \nabla'\nabla'\right]\cdot\bar{F}(\bar{r}')\,ds' \qquad (36)$$

and

$$j\omega\mu\,\bar{H}(\bar{r}) = \left[k^2\bar{\bar{I}} + \nabla\nabla\right]\cdot\bar{F}^i(\bar{r}) + \nabla\times\oint_S \Phi\,\hat{n}'\times\left[k^2\bar{\bar{I}} + \nabla'\nabla'\right]\cdot\bar{F}(\bar{r}')\,ds' + \left[k^2\bar{\bar{I}} + \nabla\nabla\right]\cdot\oint_S \Phi\,\hat{n}'\times\left[\nabla'\times\bar{F}(\bar{r}')\right]ds' \quad (37)$$

When both independent magnetic and electric sources are present, the electromagnetic field equations are

$$\bar{E}(\bar{r}) = \frac{1}{j\omega\varepsilon}\left[k^2\bar{\bar{I}} + \nabla\nabla\right]\cdot\bar{A}^i(\bar{r}) - \nabla\times\bar{F}^i(\bar{r}) + \left[k^2\bar{\bar{I}} + \nabla\nabla\right]\cdot\oint_S \Phi\,\hat{n}'\times\left\{\frac{1}{j\omega\varepsilon}\nabla'\times\bar{A}(\bar{r}') + \frac{1}{k^2}\left[k^2\bar{\bar{I}} + \nabla'\nabla'\right]\cdot\bar{F}(\bar{r}')\right\}ds' + \nabla\times\oint_S \Phi\,\hat{n}'\times\left\{\frac{1}{j\omega\varepsilon}\left[k^2\bar{\bar{I}} + \nabla'\nabla'\right]\cdot\bar{A}(\bar{r}') - \nabla'\times\bar{F}(\bar{r}')\right\}ds' \quad (38)$$

and

$$\bar{H}(\bar{r}) = \nabla\times\bar{A}^i(\bar{r}) + \frac{1}{j\omega\mu}\left[k^2\bar{\bar{I}} + \nabla\nabla\right]\cdot\bar{F}^i(\bar{r}) + \frac{1}{k^2}\left[k^2\bar{\bar{I}} + \nabla\nabla\right]\cdot\oint_S \Phi\,\hat{n}'\times\left\{\left[k^2\bar{\bar{I}} + \nabla'\nabla'\right]\cdot\bar{A}(\bar{r}') + \frac{k^2}{j\omega\mu}\nabla'\times\bar{F}(\bar{r}')\right\}ds' + \nabla\times\oint_S \Phi\,\hat{n}'\times\left\{\nabla'\times\bar{A}(\bar{r}') + \frac{1}{j\omega\mu}\left[k^2\bar{\bar{I}} + \nabla'\nabla'\right]\cdot\bar{F}(\bar{r}')\right\}ds' \quad (39)$$

Rewriting Eqs (38) and (39), one obtains

$$\bar{E}(\bar{r}) = \bar{E}^i(\bar{r}) + [k^2\bar{\bar{I}} + \nabla\nabla] \cdot \oint_S \frac{1}{j\omega\epsilon} \Phi \, \hat{n}' \times \bar{H}(\bar{r}') \, ds'$$

$$+ \nabla \times \oint_S \Phi \, \hat{n}' \times \bar{E}(\bar{r}') \, ds' \tag{40}$$

and $$\bar{H}(\bar{r}) = \bar{H}^i(\bar{r}) - [k^2\bar{\bar{I}} + \nabla\nabla] \cdot \oint_S \frac{1}{j\omega\mu} \Phi \, \hat{n}' \times \bar{E}(\bar{r}') \, ds'$$

$$+ \nabla \times \oint_S \Phi \, \hat{n}' \times \bar{H}(\bar{r}') \, ds' \tag{41}$$

where $\bar{E}^i(\bar{r})$ and $\bar{H}^i(\bar{r})$ are the incident electromagnetic fields or fields due to the independent sources.

Since the equivalent surface currents on a scatterer are given by (Ref 7:106)

$$\bar{J}^s = \hat{n}' \times \bar{H}(\bar{r}') \tag{42}$$

and $$\bar{M}^s = -\hat{n}' \times \bar{E}(\bar{r}') \tag{43}$$

the electromagnetic fields in terms of these equivalent currents are

$$\bar{E}(\bar{r}) = \bar{E}^i(\bar{r}) + [k^2\bar{\bar{I}} + \nabla\nabla] \cdot \oint_S \Phi \frac{1}{j\omega\epsilon} \bar{J}^s(\bar{r}') \, ds'$$

$$- \nabla \times \oint_S \Phi \, \bar{M}^s(\bar{r}') \, ds' \tag{44}$$

and $$\bar{H}(\bar{r}) = \bar{H}^i(\bar{r}) + [k^2\bar{\bar{I}} + \nabla\nabla] \cdot \oint_S \Phi \frac{1}{j\omega\mu} \bar{M}^s(\bar{r}') \, ds'$$

$$+ \nabla \times \oint_S \Phi \, \bar{J}^s(\bar{r}') \, ds' \tag{45}$$

If the scatterer is assumed to be a perfect electric conductor, these equations simplify to

$$\bar{E}(\bar{r}) = \bar{E}^i(\bar{r}) + [k^2 \bar{\bar{I}} + \nabla\nabla] \cdot \frac{1}{j\omega\varepsilon} \oint_S \Phi \, \bar{J}^s(\bar{r}') \, ds' \tag{46}$$

and
$$\bar{H}(\bar{r}) = \bar{H}^i(\bar{r}) + \nabla \times \oint_S \Phi \, \bar{J}^s(\bar{r}') \, ds' \tag{47}$$

since $\bar{M}^s$ is zero on a perfect electric conductor.

It should be noted that the development in this chapter used vector potentials to reduce the restrictions on the differentiability of the $\bar{E}$ and $\bar{H}$ fields; the differentiability of the integrals in Eqs (46) and (47) must still be considered when the observation point is permitted to be on the scattering surface. This point will be addressed in the last section of this chapter.

Cylinder Plus Wire Equations

Figure 2 depicts the geometry of the scattering problem considered in this thesis. The cylinder and wire (infinitesimally thin, finite, cylindrical surfaces at $\rho = a$ and $\rho = b$ respectively) are assumed to be perfect electric conductors. The wire is assumed to have a negligible radius relative to the radius of the cylinder and the wavelength of the incident field. The incident field is a plane wave assumed to be a transverse magnetic field with its propagation vector in the x-z plane at an angle θ_i with respect to the z axis as shown in the inset of Figure 2. This ensures that there will be a component of the

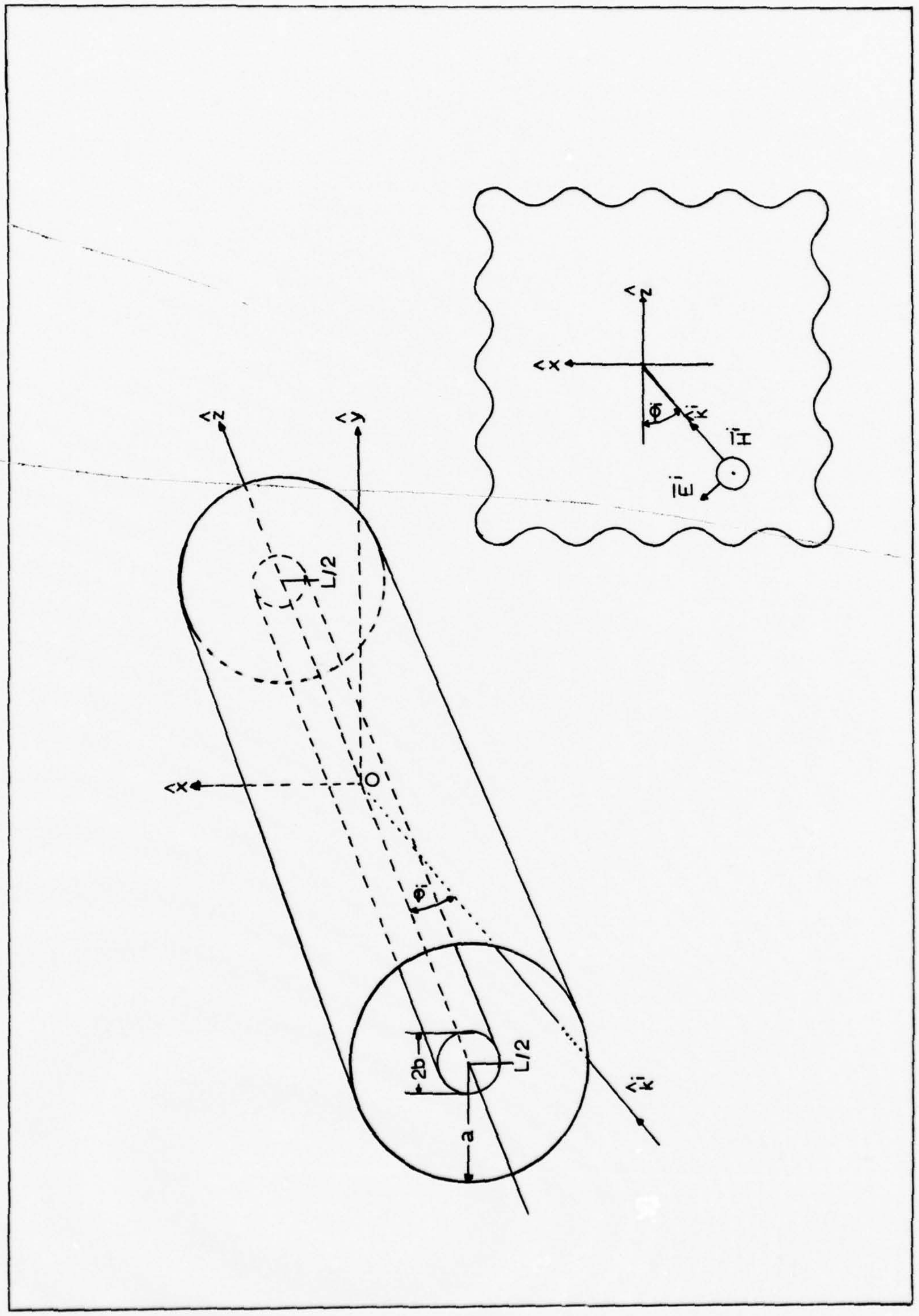

Figure 2. Cylinder Plus Wire Geometry

incident $\bar{E}$ field along the wire.

In general, the incident fields and currents for the structures of interest can be expanded in Fourier series. For plane waves, the incident $\bar{E}$ and $\bar{H}$ fields can be represented as (Ref 4:17)

$$\bar{E}^i = \sum_{n=-\infty}^{\infty} \left[\hat{\rho} E^i_{\rho_n} + \hat{\phi} E^i_{\phi_n} + \hat{z} E^i_{z_n}\right] e^{jn\phi} e^{-jkz\cos\theta_i} \tag{48}$$

and

$$\bar{H}^i = \sum_{n=-\infty}^{\infty} \left[\hat{\rho} H^i_{\rho_n} + \hat{\phi} H^i_{\phi_n} + \hat{z} H^i_{z_n}\right] e^{jn\phi} e^{-jkz\cos\theta_i} \tag{49}$$

where the coefficients are a function of ρ only and the variation with respect to z and ϕ (coordinate variation in standard cylindrical coordinates) are shown explicitly. The surface currents on the structures may similarly be expanded as

$$\bar{J}(z') = \sum_{n=-\infty}^{\infty} \left[\hat{\phi} J_{\phi_n}(z') + \hat{z} J_{z_n}(z')\right] e^{jn\phi} \tag{50}$$

It will be assumed that there is no significant ϕ variation in the surface current on the wire since its radius is negligible relative to wavelength. Therefore, the wire surface current may be represented by

$$\bar{J}^w(z') = \hat{z} J^w_{z_0}(z') \tag{51}$$

Since the $\hat{z}$ component of the incident $\bar{E}$ field is the component which induces a current on the wire, one may assume that the incident $\bar{E}$ field has only a $\hat{z}$ component which may be expanded as (Ref 4:17)

$$E_z^i = \sum_{n=-\infty}^{\infty} E_o \sin\theta_i (-j)^n J_n(k\rho \sin\theta_i) e^{jn\phi} e^{-jkz\cos\theta_i} \tag{52}$$

where E_o is the amplitude of the incident $\bar{E}$ field at the origin of the coordinate system and the J_n are Bessel functions of the first kind. The current on the cylinder contains both terms of the expansion given in Eq (50).

Davis (Ref 4), in his analysis of scattering by a finite hollow cylinder, showed that currents of harmonic n are associated with only incident fields of the same harmonic and that by symmetry only non-negative values of n need be considered. Davis's results and the fact that the objective of this thesis is to determine the effect of the wire on scattering by finite cylinders permits one to use only the zero harmonic term of the expansions for the incident field and cylinder currents since the zero harmonic behavior will be the dominant behavior, Therefore, the equations considered in this thesis for the currents on the wire and cylinder and the incident field are respectively

$$\bar{J}^w(z') = \hat{z}\, J_{z_o}^w(z') \tag{51}$$

$$\bar{J}^c(z') = \hat{z}\, J^c_{z_0}(z') + \hat{\phi}\, J^c_{\phi_0}(z') \tag{53}$$

and

$$\bar{E}^i = \hat{z}\, E_0 \sin\theta_i\, J_0(k\rho \sin\theta_i)\, e^{-jkz\cos\theta_i} \tag{54}$$

Substituting Eqs (51), (53), and (54) into Eq (46) and realizing that vector potentials only have components along the direction of their sources, one obtains

$$E_z(\bar{r}) = E_0 \sin\theta_i\, J_0(k\rho \sin\theta_i)\, e^{-jkz\cos\theta_i}$$

$$+ (k^2 + d_z^2)\frac{1}{j\omega\varepsilon} \oint_S \Phi\, J_z(z')\, ds' \tag{55}$$

where d_z is the derivative with respect to z and J_z represents the total zero harmonic z-directed surface current on the structures. The effect of the ϕ component of the cylinder current is zero since the partial derivative of $J^c_{\phi_0}(z')$ with respect to ϕ is zero.

Noting that the tangential $\bar{E}$ fields must be zero at the boundaries of perfect electric conductors, one can write the equations for the currents on the cylinder and wire as

$$-j\omega\varepsilon\, E_0\, J_0(ka \sin\theta_i)\, e^{-jkz\cos\theta_i} \sin\theta_i =$$

$$(k^2 + d_z^2)\left\{ \oint_{S_w} \Phi(a,b;z-z')\, J^w_{z_0}(z')\, ds' \right.$$

$$\left. + \oint_{S_c} \Phi(a,a;z-z')\, J^c_{z_0}(z')\, ds' \right\} \tag{56}$$

and

$$-j\omega\varepsilon E_o J_o(kb \sin\theta_i)\, e^{-jkz\cos\theta_i} \sin\theta_i =$$

$$(k^2 + d_z^2)\left\{\oint_{S_w} \Phi(b,b;z-z')\, J_{z_o}^{w}(z')\, ds' + \oint_{S_c} \Phi(a,b;z-z')\, J_{z_o}^{c}(z')\, ds'\right\} \qquad (57)$$

where a and b refer to the radii of the cylinder and wire respectively and S_w and S_c refer to the surfaces of the wire and cylinder respectively. The equation for the corresponding current on a hollow cylinder is

$$-j\omega\varepsilon E_o J_o(ka \sin\theta_i)\, e^{-jkz\cos\theta_i} \sin\theta_i =$$

$$(k^2 + d_z^2) \oint_{S_c} \Phi(a,a;z-z')\, J_{z_o}^{c}(z')\, ds' \qquad (58)$$

Kernel Evaluation

The development of the integral equations for the equivalent surface currents on a finite cylinder and wire was restricted by not permitting the observation point to be on the surfaces of the scatterers. The complete solution for the fields requires that the observation point be permitted to be on the surfaces. This presents an added difficulty since the kernel of the integrals in Eqs (56), (57), and (58) possess singularities for some observation points. If the order of integration and differentiation is interchanged in these equations, as will be done in Chapter III, the kernels have nonintegrable singularities in the

Cauchy sense for some observation points. In this section a method is discussed for extracting these singularities, thus partitioning the kernel into a term which can be treated analytically and a residue which can be integrated numerically.

The method of development in this thesis consisted of using vector potentials to derive integral equations which contained terms of the form

$$T(\rho,\rho';z-z') = (k^2+d_z^2)\oint_S \Phi(\rho,\rho';z-z')\, J(z')\, ds' \qquad (59)$$

Terms of the same form would have evolved if the development had been based on $\bar{E}$ and $\bar{H}$ (Ref 4). The vector potential method was used since its validity did not require the electromagnetic fields to be twice differentiable. However, this method does not reduce the degree of smoothness required on the kernel of Eq (59). Both methods require the same degree of smoothness of the kernel and require the extraction of the nonintegrable singularities if $T(\rho,\rho';z-z')$ is to be determined.

Davis (Ref 4:8) treated the nonintegrable singularity problem through a limiting process by letting the observation point $\bar{r}$ approach a surface point $\bar{r}'$. The surface was divided into two regions, a small patch that contained $\bar{r}'$, and the rest of the surface. That portion which excluded the small patch contained no singularities and required no special handling as $\bar{r}$ approached $\bar{r}'$. However, as $\bar{r}$ approached $\bar{r}'$ in the integral over the small patch, it was necessary to take the Hadamard principal value (finite part) of the integral (Ref 4:89). The use of the finite part of this integral is justified since the part approaching infinity cancels with the part of the integral over the curve bounding the small patch which also approaches infinity. Hence Eq (59) may be written as

$$T(\rho,\rho';z-z') = \underset{S}{⨎} (k^2 + d_z^2)\, \Phi(\rho,\rho';z-z')\, J(z')\, ds' \tag{60}$$

where the double bar through the integral sign is Davis's notation for Hadamard principal value and the order of integration and differentiation has been interchanged. The assumption that this interchange is valid is not justified here; however, it is used to illustrate a form that occurs when a valid interchange is made in Chapter III. Equation (60) contains a residue and a singularity integrable in the Hadamard sense.

One may rewrite Eq (59) as

$$T(\rho,\rho';z-z') = (k^2 + d_z^2) \int_{-\infty}^{\infty} I(z') ⨍_{-\pi}^{\pi} \frac{e^{-jkR}}{8\pi^2 R}\, d\alpha\, dz' \tag{61}$$

where

$$R = |\bar{r} - \bar{r}'| = \sqrt{(z-z')^2 + \rho^2 + \rho'^2 - 2\rho\rho'\cos\alpha} \tag{62}$$

and the bulk current I(Z') is

$$I(z') = 2\pi\rho' J(z') P_L(L/2 - |z'|) \quad , \quad P_L(z') = \begin{cases} 1 \; , \; |z'| < L/2 \\ 0 \; , \; |z'| \geq L/2 \end{cases} \tag{63}$$

and α is the angle between the vector to the observation point and the vector to the source. The bar through the integral sign implies Cauchy principal value. Consider the integral

$$K = \fint_{-\pi}^{\pi} \frac{e^{-jkR}}{8\pi^2 R} \, d\alpha \tag{64}$$

This integral gives a singular kernel about R = 0. A technique for extracting the singularity (Ref 11) is to make a transformation of the integration in α to an integration in y, where $y = 2\sqrt{\rho\rho'} \sin \alpha/2$, and then add and subtract the Jacobian of the transformation from the kernel of the integral. Operating on Eq (64) in the manner just described yields

$$K = \int_{-\pi}^{\pi} \frac{e^{-jkR} - \cos \alpha/2}{8\pi^2 R} d\alpha + \int_{-2\sqrt{\rho\rho'}}^{2\sqrt{\rho\rho'}} \frac{1}{8\pi^2\sqrt{\rho\rho'}} \quad \frac{dy}{\sqrt{y^2 + (z-z')^2 + (\rho-\rho')^2}} \tag{65}$$

The first integral in Eq (65) is nonsingular and can be integrated numerically, and the second integral can be integrated in closed form to obtain (Ref 5:150)

$$K_1 = \frac{1}{8\pi^2\sqrt{\rho\rho'}}\left[\ln\left(2\sqrt{\rho\rho'} + \sqrt{(z-z')^2 + (\rho+\rho')^2}\right)\right.$$

$$\left. - \ln\left(-2\sqrt{\rho\rho'} + \sqrt{(z-z')^2 + (\rho+\rho')^2}\right)\right] \qquad (66)$$

For the geometry considered in this thesis, one must evaluate K_1 where $\sqrt{\rho\rho'}$ approaches zero. To facilitate this evaluation on a digital computer, one rewrites K_1 as

$$K_1 = \frac{1}{8\pi^2\sqrt{\rho\rho'}}\left[\ln\left(1 + \frac{\sqrt{\rho\rho'}}{\sqrt{(z-z')^2+(\rho+\rho')^2}}\right)\right.$$

$$\left. - \ln\left(1 - \frac{\sqrt{\rho\rho'}}{\sqrt{(z-z')^2+(\rho+\rho')^2}}\right)\right] \qquad (67)$$

Expanding the natural logarithms in Taylor series yields

$$K_1 = \frac{1}{8\pi^2}\sum_{i=1}^{\infty}\frac{2}{2i+1}\;\frac{(\rho\rho')^{i-1}}{\left[(z-z')^2+(\rho+\rho')^2\right]^{\frac{2i-1}{2}}} \qquad (68)$$

Thus, one obtains

$$T(\rho,\rho';z-z') = \int_{-\pi}^{\pi}\frac{e^{-jkR} - \cos\alpha/2}{8\pi^2 R}\,d\alpha$$

$$+ \frac{1}{8\pi^2\sqrt{\rho\rho'}}\ln\left(2\sqrt{\rho\rho'} + \sqrt{(z-z')^2+(\rho+\rho')^2}\right)$$

$$- \frac{1}{8\pi^2\sqrt{\rho\rho'}}\ln\left(-2\sqrt{\rho\rho'} + \sqrt{(z-z')^2+(\rho+\rho')^2}\right) \qquad (69)$$

or $$T(\rho,\rho';z-z') = \int_{-\pi}^{\pi} \frac{e^{-jkR} - \cos\alpha/2}{8\pi^2 R}\, d\alpha$$

$$+ \frac{1}{8\pi^2} \sum_{i=1}^{\infty} \frac{(\rho\rho')^{i-1}}{\left[(z-z')^2 + (\rho+\rho')^2\right]^{\frac{2i-1}{2}}} \; \frac{2}{2i+1} \qquad (70)$$

when $\sqrt{\rho\rho'}$ approaches zero.

Applying the results of the kernel evaluation, the equations for scattering currents on the cylinder and wire are

$$-j\omega\varepsilon E_o J_o(ka \sin\theta_i)\, e^{-jkz\cos\theta_i} \sin\theta_i =$$

$$(k^2 + d_z^2) \int_{-\infty}^{\infty} \left\{ I^c(z') \left[\int_{-\pi}^{\pi} \frac{e^{-jkR(a,a)} - \cos\alpha/2}{8\pi^2 R(a,a)}\, d\alpha + K_1(a,a) \right] \right.$$

$$\left. + I^w(z') \left[\int_{-\pi}^{\pi} \frac{e^{-jkR(a,b)} - \cos\alpha/2}{8\pi^2 R(a,b)}\, d\alpha + K_1(a,b) \right] \right\} dz' \qquad (71)$$

and

$$-j\omega\varepsilon E_o J_o(kb \sin\theta_i)\, e^{-jkz\cos\theta_i} \sin\theta_i =$$

$$(k^2 + d_z^2) \int_{-\infty}^{\infty} \left\{ I^c(z') \left[\int_{-\pi}^{\pi} \frac{e^{-jkR(a,b)} - \cos\alpha/2}{8\pi^2 R(a,b)}\, d\alpha + K_1(a,b) \right] \right.$$

$$\left. + I^w(z') \left[\int_{-\pi}^{\pi} \frac{e^{-jkR(b,b)} - \cos\alpha/2}{8\pi^2 R(b,b)}\, d\alpha + K_1(b,b) \right] \right\} dz' \qquad (72)$$

where a and b are the radii of the cylinder and wire respectively and $I^c(z')$ and $I^w(z')$ are the total currents on the cylinder and wire respectively. The expression for the zero harmonic current on a hollow cylinder is obtained by setting $I^w(z')$ equal to zero, yielding

$$
-j\omega\varepsilon E_o J_o(ka \sin\theta_i) e^{-jkz\cos\theta_i} \sin\theta_i =
$$

$$
(k^2 + d_z^2) \int_{-\infty}^{\infty} I^c(z') \left[\int_{-\pi}^{\pi} \frac{e^{-jkR(a,a)} - \cos\alpha/2}{8\pi^2 R(a,a)} d\alpha \right.
$$

$$
\left. + K_1(a,a) \right] dz' \tag{73}
$$

In the case of scattering by the wire and cylinder there are two equations and two unknowns, $I^c(z')$ and $I^w(z')$. The case of scattering by the hollow cylinder has one equation and one unknown $I^c(z')$. Since these equations cannot be solved analytically, an alternate method must be used to obtain an approximate answer. Chapter III discusses one method of obtaining approximate solutions for equations of this type.

III. Numerical Development

The solution of the scattering problem considered by this thesis requires determining unknowns that appear in the kernels of singular integral equations. One method for solving linear equations of this type is the method of moments. This process requires expanding the unknown function in terms of a set of expansion or basis functions. Each term in the set is operated on in the same manner as was the unknown function. A matrix equation involving the coefficients of the expansion can be found by taking the moment of the forcing function and of the operation on each expansion term with respect to the members of a set of weighting functions. This chapter includes a brief description of method of moments and develops digitized forms of Eqs (71) through (73) which can be solved on a digital computer. The material presented in this chapter is based on the work of Harrington (Ref 6) and Davis (Ref 4).

Method of Moments

Consider the linear operator equation

$$L u = f \tag{74}$$

where L is a linear operator, u is an unknown function, and f is a known forcing function. If the solution to Eq (74) is unique and exists for all f, one can write

$$u = L^{-1} f \tag{75}$$

where L^{-1} is the inverse operator and it is assumed that the domain of L and u and the range of f are defined over appropriate spaces.

To solve Eq (75) by using the method of moments, expand u in terms of a complete set of expansion functions u_n

$$u = \sum_{N} a_N u_N \tag{76}$$

where the a_n are the expansion coefficients. In computer applications, the summation is truncated and Eq (76) becomes

$$u = \sum_{N=1}^{N} a_N u_N + e \tag{77}$$

where e is the truncation error. Equation (74) can be written as

$$\sum_{N=1}^{N} a_N L u_N = f - Le \tag{78}$$

If one defines the interproduct of two functions h_1 and h_2 as

$$\langle h_1, h_2 \rangle = \int_{x_1}^{x_2} h_1(x)\, h_2(x)\, dx \tag{79}$$

and defines a suitable set of weighting functions w_m, m = 1,2,3,...,M, Eq (79) can be expressed as

$$\sum_{N=1}^{N} a_N \langle w_m, L u_N \rangle = \langle w_m, f \rangle - \langle w_m, Le \rangle \tag{80}$$

If the scalars $\langle w_m, Le \rangle$ are set equal to zero for each m, Eq (80) reduces to

$$\sum_{N=1}^{N} a_N \langle w_m, L u_N \rangle = \langle w_m, f \rangle \tag{81}$$

or in matrix notation

$$\left[l_{mN} \right] \left[a_N \right] = \left[f_m \right] \tag{82}$$

where

$$l_{mN} = \langle w_m, L u_N \rangle \tag{83}$$

and $$f_m = \langle w_m, f \rangle \tag{84}$$

If M = N and l_{mn} is nonsingular, the solution of this matrix equation is

$$\left[a_N \right] = \left[l_{mN} \right]^{-1} \left[f_m \right] \tag{85}$$

and the unknown u is approximated by

$$u = \left[u_N \right] \left[a_N \right] \tag{86}$$

where

$$\left[u_N \right] = \left[u_1, u_2, \ldots, u_N \right] \tag{87}$$

Therefore, the approximate solution may be written as

$$u = \left[u_N\right] \left[l_{mN}\right]^{-1} \left[f_m\right] \tag{88}$$

An appropriate set of expansion functions and weighting functions must be chosen before Eq (88) can be applied to Eqs (71) through (73). Davis (Ref 3:39) suggests that the generalized spline

$$I_N(z') = \sin k\left(\Delta - |z' - z_N|\right) P_{2\Delta}(z' - z_N) \tag{89}$$

where $z_N = N\Delta$

$$P_{2\Delta}(z' - z_N) = \begin{cases} 1, & |z' - z_N| < \Delta \\ 0, & |z' - z_N| \geq \Delta \end{cases} \tag{90}$$

is an advantageous choice for the expansion function in problems of this type and that

$$w_m = P_\Delta(z' - z_m) \quad , \quad z_m = m\Delta \tag{91}$$

are appropriate weighting functions.

Digitized Equations

Using the expansion function of Eq(89), the currents on the wire and cylinder can be approximated by

$$I_z^w(z') = \sum_{N=1}^{N} I_N^w \sin k\left(\Delta - |z' - z_N|\right) P_{2\Delta}(z' - z_N) \tag{92}$$

and

$$I_z^c(z') = \sum_{n=1}^{N} I_n^c \;\sin k\left(\Delta - |z'-z_n|\right) P_{z\Delta}(z'-z_n) \tag{93}$$

where $\Delta = \dfrac{L}{N+1}$.

Substituting Eqs (92) and (93) into the scattering current equations derived in the previous section, one obtains equations of the form

$$-j\omega\varepsilon E_0 J_0(ka \sin\theta_i)\, e^{-jkz\cos\theta_i} \sin\theta_i =$$

$$\fint_{-\infty}^{\infty} \Big\{ (k^2 + d_z^2) \Big[G(a,a;z-z') \sum_{n=1}^{N} I_n^c \sin k\left(\Delta - |z'-z_n|\right) P_{z\Delta}(z'-z_n)$$

$$+ G(a,b;z-z') \sum_{n=1}^{N} I_n^w \sin k\left(\Delta - |z'-z_n|\right) P_{z\Delta}(z'-z_n) \Big] \Big\}\, dz' \tag{94}$$

where the Hadamard form has been used as a result of the interchange of the integration in z' and the operation $(k^2 + d_z^2)$ and

$$G(a,b;z-z') = \int_{-\pi}^{\pi} \frac{e^{-jkR(a,b)} - \cos\alpha/2}{8\pi^2 R(a,b)}\, d\alpha + K_1(a,b) \tag{95}$$

Equation (94) can be integrated by parts twice with respect to z' to obtain an equation of the form

$$-j\omega\varepsilon E_o J_o(ka \sin\theta_i) e^{-jkz\cos\theta_i} \sin\theta_i =$$

$$\int_{-\infty}^{\infty} \Big\{ G(a,a;z-z') (k^2+d_{z'}^2) \sum_{N=1}^{N} I_N^c \sin k(\Delta-|z'-z_N|) P_{2\Delta}(z'-z_N)$$

$$+ G(a,b;z-z') (k^2+d_{z'}^2) \sum_{N=1}^{N} I_N^w \sin k(\Delta-|z'-z_N|) P_{2\Delta}(z'-z_N) \Big\} dz' \qquad (96)$$

where the operation

$$Q = (k^2+d_{z'}^2) \sum_{N=1}^{N} I_N^c \sin k(\Delta-|z'-z_N|) P_{2\Delta}(z'-z_N) \qquad (97)$$

may be taken analytically to give

$$Q = \sum_{N=1}^{N} k I_N^c \left[\delta(z'-z_{N+1}) + \delta(z'-z_{N-1}) - 2\cos(k\Delta)\,\delta(z'-z_N) \right] \qquad (98)$$

To complete the method of moments, one takes the inner product of the pulse weighting functions and Eq (96) and the similar equation that represents the evaluation of the boundary condition at the wire. Operating on the forcing functions yields

$$f_m(a) = -\int_{m\Delta-\Delta/2}^{m\Delta+\Delta/2} j\omega\varepsilon E_o (ka \sin\theta_i) e^{-jkz\cos\theta_i} \sin\theta_i \, dz \qquad (99)$$

and

$$f_m(b) = -\int_{m\Delta-\Delta/2}^{m\Delta+\Delta/2} j\omega\varepsilon E_o J_o(kb \sin\theta_i) e^{-jkz\cos\theta_i} \sin\theta_i \, dz$$

Similar operations on the right hand side of Eq (96) results in a set of 2M linear equations for the 2N unknown current coefficients. These equations have the form

$$f_m(a) = \sum_{N=1}^{N} k I_N^c \left[G_{m,N+1}(a,a) + G_{m,N-1}(a,a) - 2\cos(k\Delta) G_{m,N}(a,a)\right]$$

$$+\sum_{N=1}^{N} k I_N^w \left[G_{m,N+1}(a,b) + G_{m,N-1}(a,b) - 2\cos(k\Delta) G_{m,N}(a,b)\right]$$

and

$$f_m(b) = \sum_{N=1}^{N} k I_N^w \left[G_{m,N+1}(b,b) + G_{m,N-1}(b,b) - 2\cos(k\Delta) G_{m,N}(b,b)\right]$$

$$+\sum_{N=1}^{N} k I_N^c \left[G_{m,N+1}(a,b) + G_{m,N-1}(a,b) - 2\cos(k\Delta) G_{m,N}(a,b)\right]$$

where

$$G_{mN}(\rho_1,\rho_2)=\int_{m\Delta-\Delta/2}^{m\Delta+\Delta/2}\int_{-\infty}^{\infty} G(\rho_1,\rho_2;z-z')\,\delta(z'-z_N)\,dz'\,dz \tag{103}$$

for the cylinder plus wire problem. These equations can be written in matrix notation as

$$\begin{bmatrix} f_1(a) \\ \vdots \\ f_M(a) \\ f_1(b) \\ \vdots \\ f_M(b) \end{bmatrix} = \left[\begin{array}{c|c} l_{m,N}(a,a) & l_{m,N}(a,b) \\ \hline l_{m,N}(a,b) & l_{m,N}(b,b) \end{array}\right] \begin{bmatrix} I_1^c \\ \vdots \\ I_M^c \\ I_1^w \\ \vdots \\ I_M^w \end{bmatrix} \tag{104}$$

where

$$l_{m,N}(a,b) = \left[G_{m,N+1}(a,b) + G_{m,N-1}(a,b) - 2\cos(k\Delta)\,G_{m,N}(a,b)\right] \tag{105}$$

The resultant solution for the current coefficients is

$$\begin{bmatrix} I_1^c \\ \vdots \\ I_M^c \\ I_1^w \\ \vdots \\ I_M^w \end{bmatrix} = \left[\begin{array}{c|c} l_{m,N}(a,a) & l_{m,N}(a,b) \\ \hline l_{m,N}(a,b) & l_{m,N}(b,b) \end{array}\right]^{-1} \begin{bmatrix} f_1(a) \\ \vdots \\ f_M(a) \\ f_1(b) \\ \vdots \\ f_M(b) \end{bmatrix} \tag{106}$$

if the matrix is nonsingular and invertible. The solution for the hollow cylinder problem is

$$\begin{bmatrix} I_1^c \\ \cdot \\ \cdot \\ \cdot \\ I_M^c \end{bmatrix} = \begin{bmatrix} & & \\ & l_{m,n}(a,a) & \\ & & \end{bmatrix}^{-1} \begin{bmatrix} f_1(a) \\ \cdot \\ \cdot \\ \cdot \\ f_M(a) \end{bmatrix} \tag{107}$$

where $l_{mn}(a,a)$ and $f_m(a)$ are defined in the same manner as the definitions in the cylinder plus wire problem.

Expressions for the total electric field can be written in terms of these unknown currents. Consider the z component of the electric field.

$$E_z = E_z^i + E_z^s(a) \quad E_z^s(b) \tag{108}$$

where $E_z^S(a)$ and $E_z^S(b)$ are components of the field scattered by the structures at radii a and b respectively. The field scattered by the structure at radius a is given by

$$j\omega\varepsilon\, E_z^s(a) = (k^2 + \partial_z^2) \oint_S \Phi\, J_z^c \, ds' \tag{109}$$

Noting that this equation is of the same form as was the equation that had to be solved in determining the currents, one can write

$$E^s_{z_N}(\bar{r}) = j\eta \; I^c_N \left[G_{N+1}(\rho,a) + G_{N-1}(\rho,a) - 2\cos(k\Delta)\, G_N(\rho,a)\right]$$

$$+ \, j\eta \, I^w_N \left[G_{N+1}(\rho,b) + G_{N-1}(\rho,b) - 2\cos(k\Delta)\, G_N(\rho,b)\right] \tag{110}$$

where the n indexes the components due to the n^{th} expansion function of the currents or the components due to the current on each of the N divisions of the structures in the z dimension and η is the impedance of the medium. The total $E^s_z(\bar{r})$ is given by a summation over n for both structures or

$$E^s_z(\bar{r}) = \left[I_N(a)\right]\left[I^c_N\right] + \left[I_N(b)\right]\left[I^w_N\right] \tag{111}$$

where the

$$I_N(a) = j\eta \left[G_{N+1}(\rho,a) + G_{N-1}(\rho,a) - 2\cos(k\Delta)\, G_N(\rho,a)\right] \tag{112}$$

and n = 1,2,3,...,N.

An expression for the $\hat{\rho}$ component of the electric field can be derived using Eq (4), the equation for the divergence of $\bar{E}$, yielding

$$\frac{1}{\rho}\frac{\partial(\rho E_\rho)}{\partial \rho} + \frac{1}{\rho}\frac{\partial E_\phi}{\partial \phi} + \frac{\partial E_z}{\partial z} = \frac{\rho_e}{\varepsilon} \tag{113}$$

When the observation point is on the wire, Eq (113) can be written as

$$\frac{1}{\rho}\frac{\partial(\rho E_\rho)}{\partial\rho} = \frac{\rho_e^w}{\varepsilon} \tag{114}$$

since E_z is zero at the surface and E_ϕ is always zero for the geometry considered in this thesis. Using Eq (6), the current continuity equation, one can write

$$\frac{1}{\rho}\frac{\partial(\rho E_\rho)}{\partial\rho} = \frac{j\eta}{k2\pi\rho}\frac{\partial[I_z^w(z')]}{\partial z}\delta(\rho-b) \tag{115}$$

about the radius $\rho = b$. Integrating from $\rho = b^-$ to $\rho = b^+$ yields

$$b^+E_\rho(b^+) - b^-E_\rho(b^-) = \frac{j\eta}{k2\pi}\frac{\partial[I_z^w(z')]}{\partial z} \tag{116}$$

and $E_\rho(b)$ becomes

$$E_\rho(b^+) = \frac{b^-E_\rho(b^-)}{b^+} + \frac{j\eta}{k2\pi b^+}\frac{\partial[I_z^w(z')]}{\partial z} \tag{117}$$

Assuming that E_ρ is zero inside the wire, $\rho < b$,

$$E_\rho(b)\Big|_{z=N\Delta} = \frac{j\eta}{k2\pi b}\frac{I_{N+1}^w - I_{N-1}^w}{2\Delta}\sin(k\Delta) \tag{118}$$

where central differences about $z = n\Delta$ has been used to obtain $\frac{\partial [I_z^w(z')]}{\partial z}$. Likewise, E_ρ for $\rho = a$ is

$$E_\rho(a^+)\Big|_{z=N\Delta} = \frac{a^- E_\rho(a^-)}{a^+} + \frac{j\eta}{k 2\pi a^+} \frac{I^c_{N+1} - I^c_{N-1}}{2\Delta} \sin(k\Delta) \tag{119}$$

or

$$E_\rho(a)\Big|_{z=N\Delta} = E_\rho(a^-) + \frac{j\eta}{k 2\pi a} \frac{I^c_{N+1} - I^c_{N-1}}{2\Delta} \sin(k\Delta) \tag{120}$$

For observation points not on either surface

$$\frac{1}{\rho} \frac{\partial(\rho E_\rho)}{\partial \rho} = -\frac{\partial E_z}{\partial z} \tag{121}$$

which may be written in difference form as

$$\frac{\rho_2 E_\rho(\rho_2) - \rho_1 E_\rho(\rho_1)}{\rho_2 - \rho_1} = -\rho \frac{[E_z(z_2) - E_z(z_1)]}{z_2 - z_1}, \; z_2 - z_1 = 2\Delta \tag{122}$$

or

$$E_\rho(\bar{r}_2) = \frac{\rho_1 E_\rho(\bar{r}_1)}{\rho_2} - \frac{(\rho_2 - \rho_1)}{\rho_2} \rho \frac{E_z(z_2) - E_z(z_1)}{2\Delta} \tag{123}$$

The term

$$\rho \frac{\partial E_z}{\partial z} = \rho \frac{E_z(z_2) - E_z(z_1)}{2\Delta} \tag{124}$$

must be interpreted in some manner with respect to ρ. Since a difference form was used on $\frac{\partial(\rho E_\rho)}{\partial \rho}$, one interpretation is to use an average with respect to ρ to give

$$\rho \frac{\partial E_z}{\partial z} = \frac{\rho_2 \left[E_{z_{n+1}}(\rho_2) - E_{z_{n-1}}(\rho_2) \right] + \rho_1 \left[E_{z_{n+1}}(\rho_1) - E_{z_{n-1}}(\rho_1) \right]}{4\Delta} \quad (125)$$

In this chapter, equations that can be solved digitally have been developed for the unknown scattering currents. Additional equations were developed for the components of the total electric field in terms of these scattering currents and the incident field. Chapter IV describes some of the specific structural dimensions that have been simulated on a digital computer and the results of these simulations.

IV. Results

The objective of this thesis was to determine the effect of placing a second scatterer inside of a finite circular cylinder. Two computer programs were written to provide data for this analysis. One program computed the zero harmonic z-directed currents and the electric field components for a hollow cylinder. The second program computed the same quantities for a cylinder of the same dimensions as the hollow cylinder; however, a wire was placed on its longitudinal axis. The programs were run for structures of various dimensions in an effort to provide data which demonstrates the validity of the development and programming as well as data which would be useful in analyzing practical scattering problems. The output included plots of the incident $\bar{E}$ field, the z-directed currents on the structures, and the total electric field components for five different z planes.

Validation Data

Although all results were analyzed for effects that differed from what one would expect, two specific geometries were simulated to check the validity of this work. The first case simulated a cylinder whose radius, a, made the product ka equal to the first zero of the zero order Bessel function of the first kind. The second case simulated a long thin cylinder.

One can readily analyze the effect of the cylinder by selecting ka to be equal to the first zero of $J_0(k\rho)$ and assuming normal incidence. As would be expected, there was no scattering from the hollow cylinder since the forcing function was zero at the surface. The cylinder current was zero and the total field was equal to the incident field. Adding the wire to the geometry modified the results. In addition to the current induced on the wire, a small current was induced on the cylinder by the field scattered by the wire. The total scattered fields, composed of a tangential component E_z and radial component E_ρ, were non-zero with the wire present.

Harrington (7:233) analyzed scattering by an infinite cylinder, assuming normal TM incidence, and derived the equation

$$J_z = -\frac{2E_0}{\omega\mu\pi a}\frac{1}{H_0^{(2)}(ka)} \tag{126}$$

for the zero harmonic current density induced on the cylinder where $H_0^{(2)}(ka)$ is the zero order Hankel function of the second kind. Figure 3 illustrates the magnitude of the current computed by the program for a hollow structure with a radius of 0.01 wavelength and a length of five wavelengths and the magnitude of the currents computed by using Eq(133). The amplitude variations of the program computed current are due to the end effects associated with a finite structure.

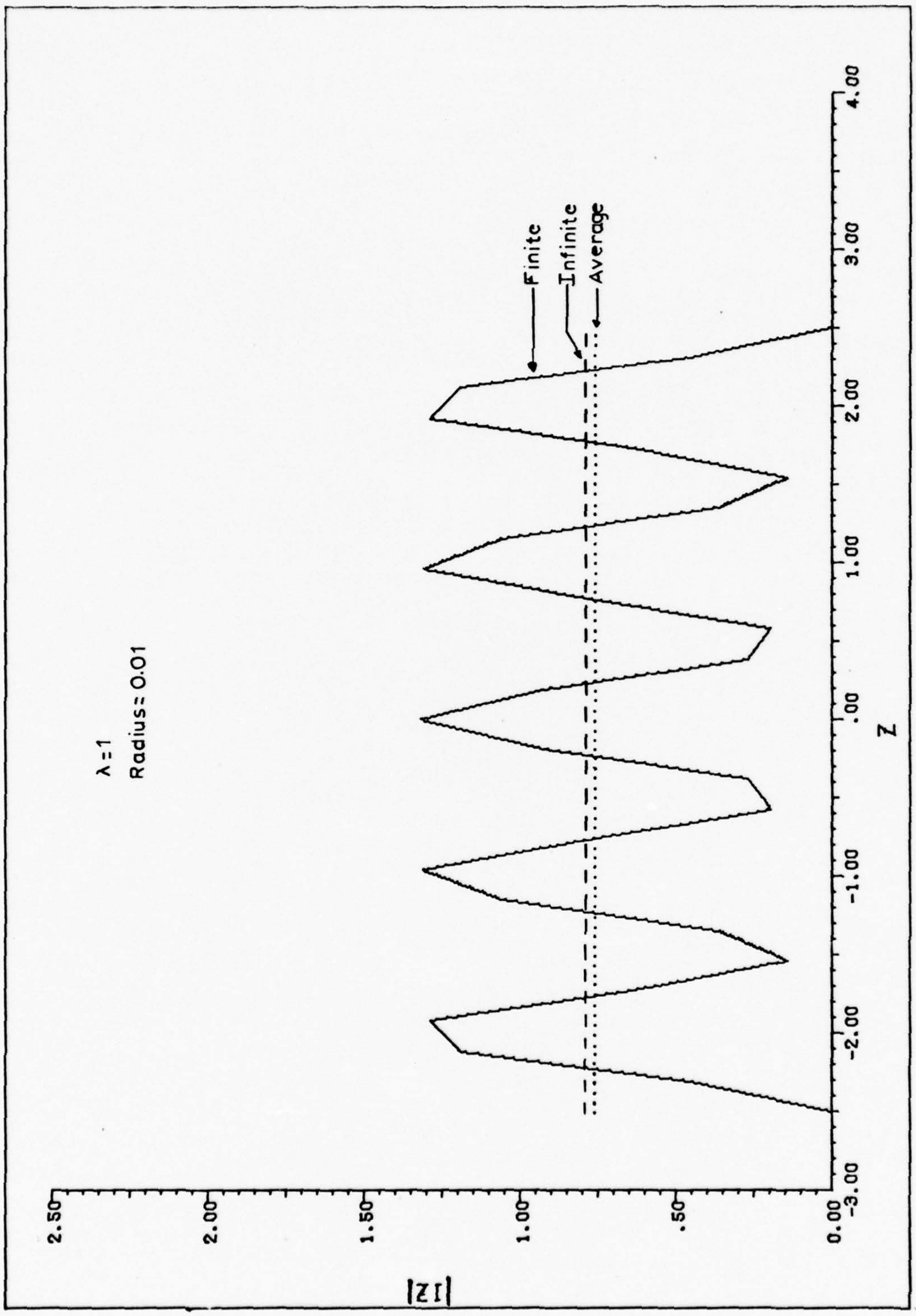

Figure 3. Magnitude of I_z for Infinite and Long Finite Cylinders

If one takes the average of the amplitude variations, there is good agreement with Harrington's current on an infinite cylinder. Figure 4 shows Harrington's solution for E_z of an infinite cylinder and the program solution for E_z in a plane mid-way between the ends of the cylinder. As one can see, there is no noticeable difference in the fields. Comparing these results to the results for shorter cylinders, the convergence of the program solutions toward the infinite cylinder solution was observed as the length increased.

Practical Data

The sponsors of this thesis are interested in predicting the scattering effects from complex structures such as an aircraft with its myriad of cables, compartments, equipment, and apertures. In an effort to provide data that might give insight into scattering problems of this type, three sets of dimensions were selected that simulate physical structures being irradiated by a TM wave of unit magnitude. The wavelength of the incident field was selected to be in the middle of the VHF band at 30 meters.

The first structure simulated was a coaxial transmission line whose outer radius was three-eighths (3/8) inch and inner radius was one-eighth (1/8) inch. The bulk current on the outer conductor was three orders of magnitude greater than the bulk current on the inner

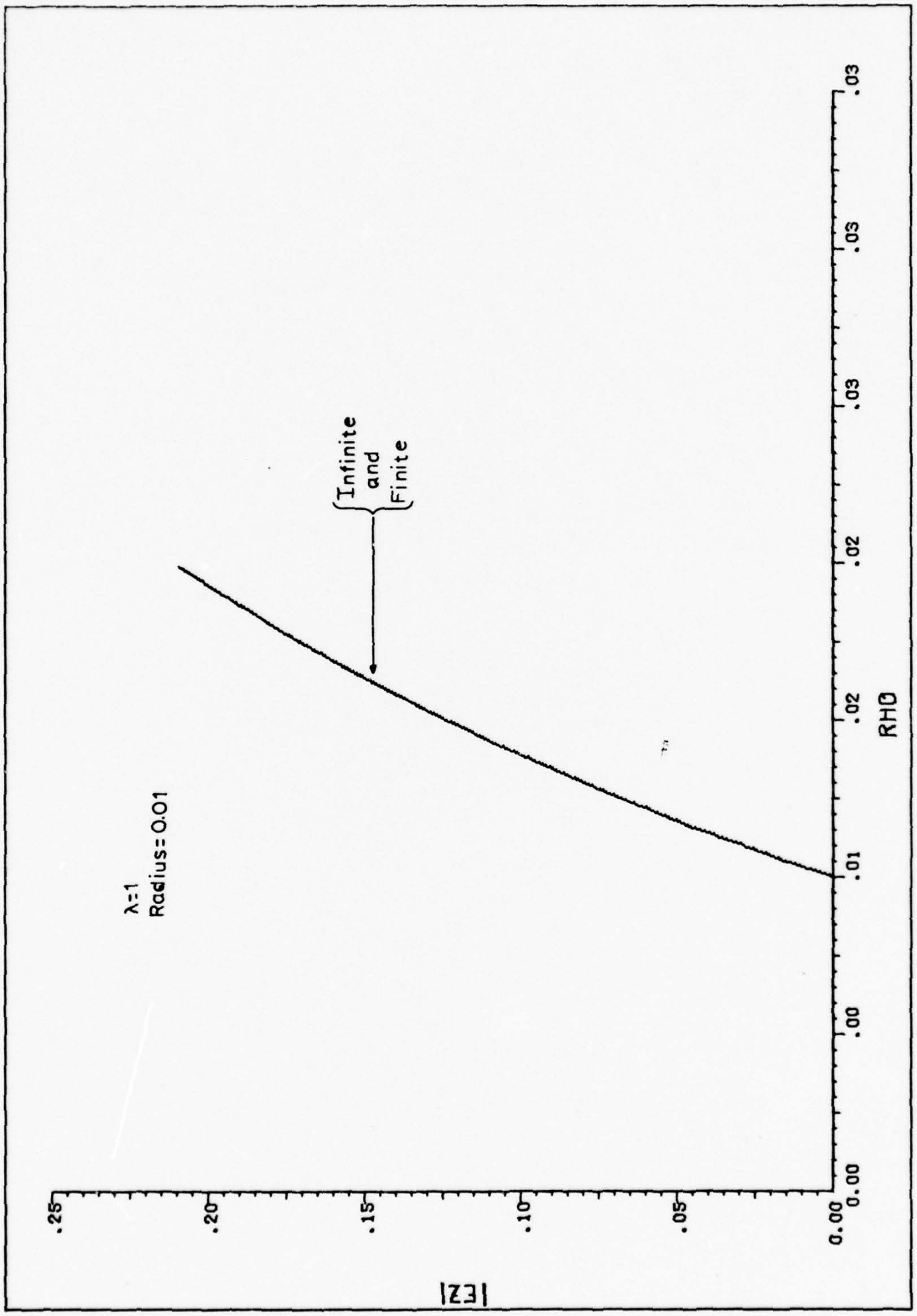

Figure 4. Magnitude of E_z for Infinite and Long Finite Cylinders

conductor. Comparing the coaxial transmission line to a hollow cylinder (circular waveguide) with the same outer radius, one finds that the z-component of the electric field inside the coaxial line is three orders of magnitude smaller than the corresponding component in the hollow cylinder; whereas the radial component of the electric field inside the coaxial line is three orders of magnitude greater than the corresponding component in the hollow cylinder. Although the magnitude of the total current on the coaxial line was approximately equal to the magnitude of the current of the hollow cylinder, the interior field structures were significantly different.

The second structure simulated was a tunnel, radius eight feet, with a conduit, radius two and one-half inches, on its central axis. The length of the tunnel was selected to be 75 meters. Figure 5 depicts the magnitude of E_z for the hollow tunnel and tunnel plus conduit as a function of radius in a plane approximately 9 meters into the tunnel. One can see that there is no noticeable difference in the two cases and that E_z is approximately zero inside the tunnels (radii less than 2.4 meters). Figure 6 depicts the magnitude of the radius times the radial component of the electric field as a function of radius for the same z. One can see that the hollow tunnel has no appreciable field inside the structure; however, the tunnel with the conduit along its central axis has a significant radial electric field in its interior.

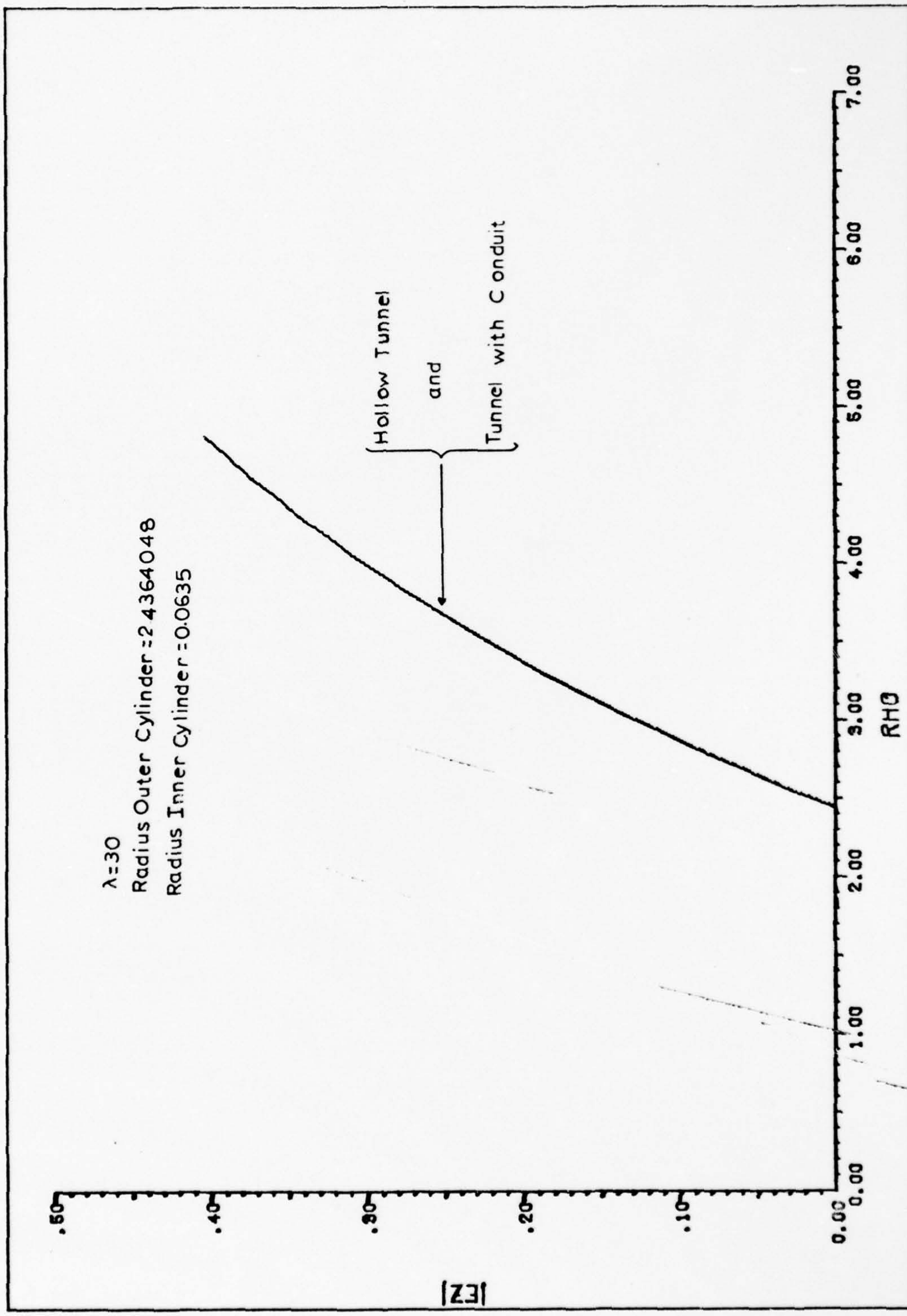

Figure 5. Magnitude of E_z for Simulated Tunnels

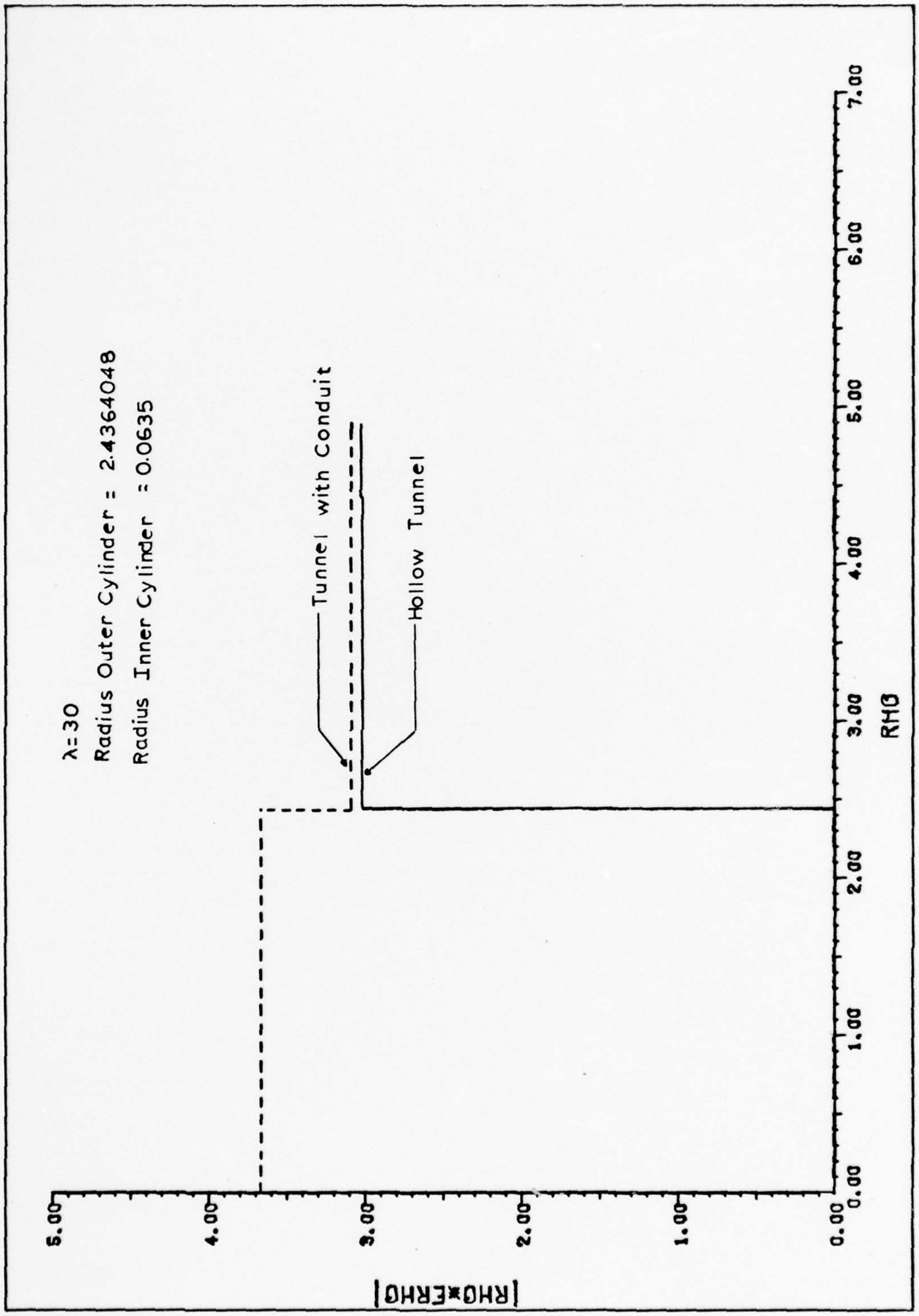

Figure 6. Magnitude of $\rho \times E_\rho$ for Simulated Tunnels

The third physical structure simulated was a large aircraft or missile with a radius of approximately six meters and a length of seventy-five meters. Figure 7 depicts E_z for a z-plane approximately 19 meters from the end of the structure. There is no noticeable difference between the hollow structure and the structure which had a 0.3 centimeter radius wire on its axis. Figure 8 depicts the magnitude of radius times the radial component of the electric field for the hollow structure and the structure with the wire in the same z-plane. Again, there is a significant radial component inside the structure with the wire; whereas, the hollow structure radial component is approximately zero.

Ten additional simulations were made in which the parameters wavelength, physical size, and the angle of incidence were varied. In general, the results were similar to the results described in previous paragraphs. An exception occurred when the length of the concentric cylinder structures was selected to be less than 1/2 wavelength long and the radii of the outer cylinder and inner cylinder were selected to be 0.1 and 0.0001 wavelengths respectively. Figure 9 depicts E_z in a z-plane approximately three-sixteenths (3/16) of a wavelength from the middle of the structures. One structure is 0.5 wavelength long and the other is 0.4 wavelength long. It can be seen that there is a marked difference in the two curves. The magnitudes of the currents

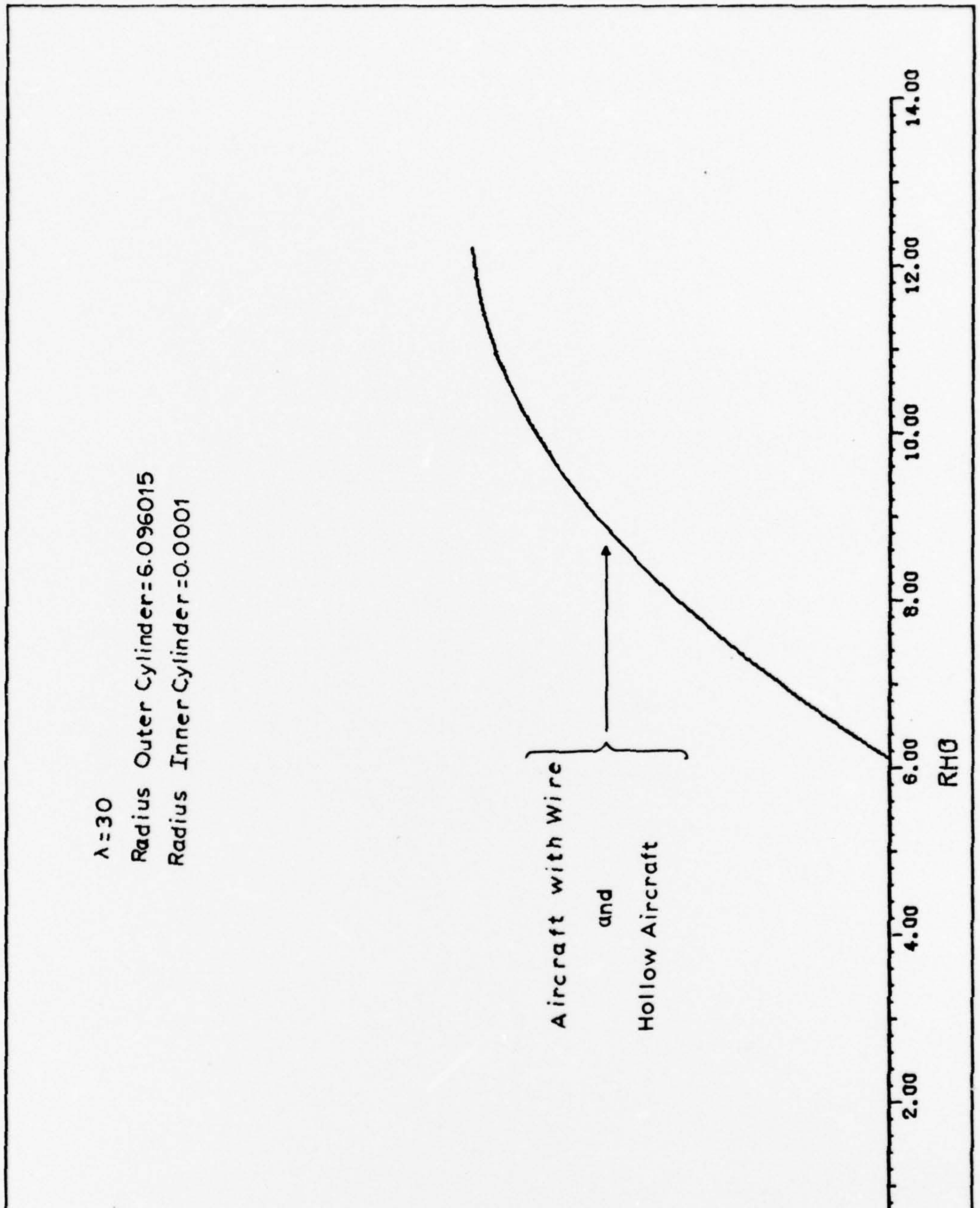

Figure 7. Magnitude of E_z for Simulated Aircraft

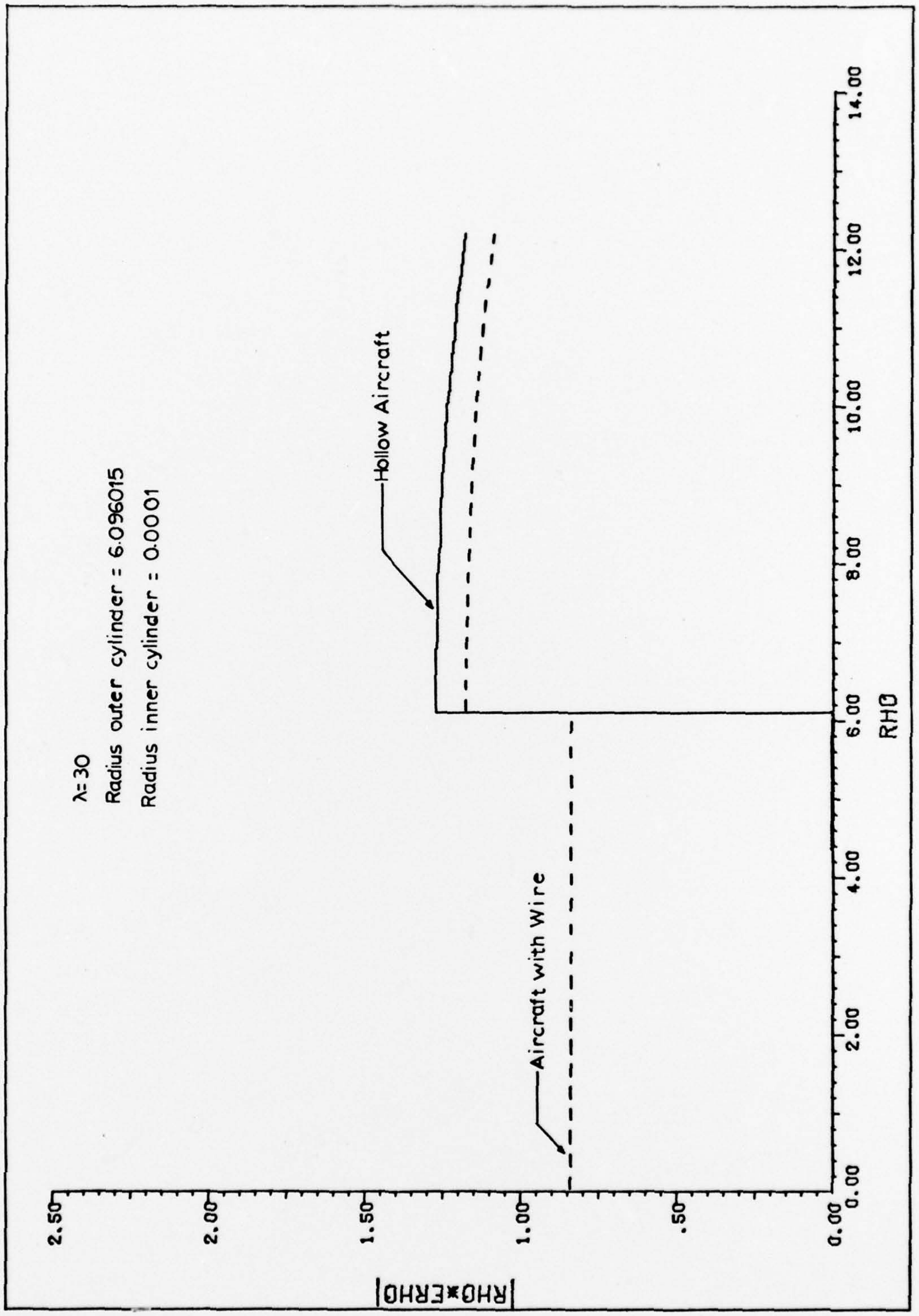

Figure 8. Magnitude of $\rho x E_\rho$ for Simulated Aircraft

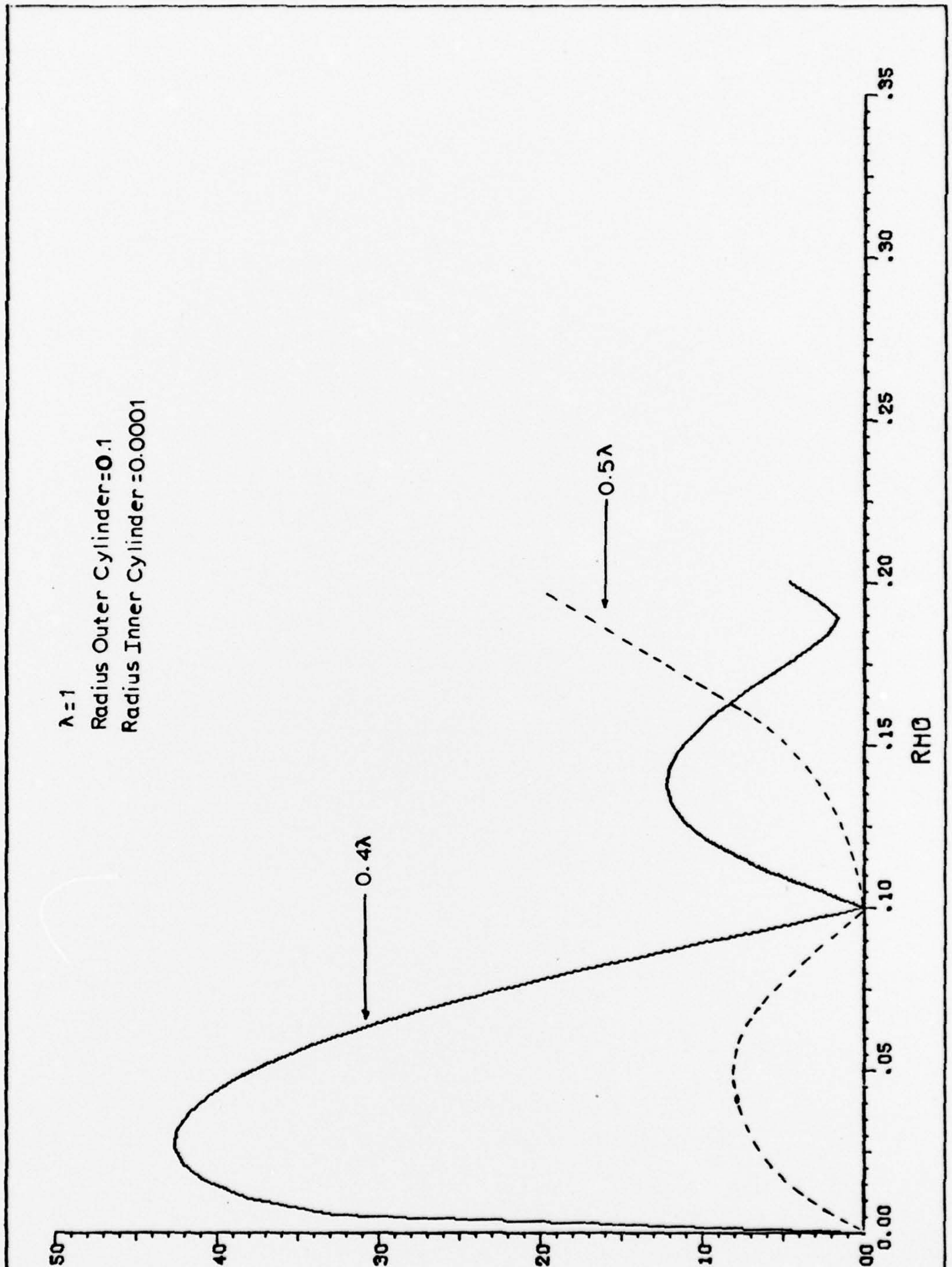

Figure 9. Magnitude of E_z for 0.4λ and 0.5λ Coaxial Cylinders with Identical Radii

on the outer conductors for the two cases were approximately equal; however, the magnitude of the current on the inner conductor of the shorter structure was approximately five times the magnitude of the current on the inner conductor of the longer structure. These results suggest some type of TM modal structure for the fields in the shorter structure and a TEM modal structure for the fields in the longer structure.

V. Conclusions and Recommendations

This thesis addressed electromagnetic scattering by two concentric, finite length, circular, perfect electric conductors. Total electromagnetic field equations were derived in terms of vector potentials. This permits one to lower the degree of differentiability required on the electromagnetic fields as opposed to what is required when the total fields are derived in terms of the electromagnetic field components. The total field equations were manipulated to yield integral equations for the equivalent surface currents induced on the cylinders by the incident fields. The method of moments was used to formulate digitized equations that could be solved on a digital computer for the unknown currents. Digitized equations were derived for the tangential and radial components of the scattered electric field. Several comparisons were made between the scattering from a finite hollow cylinder and the two cylinder case.

A conclusion that must be drawn from this analysis is that introducing the second conductor into the problem significantly changed the scattering problem. While the magnitudes of the zero harmonic currents on the hollow conductor and the outer conductor of the concentric case were approximately equal, the effect of a small radius inner conductor cannot be ignored. The modal structure of the fields between the concentric conductors is significantly different from the modal structure of a hollow conductor of similar dimensions. If one desires to analyze the fields between two concentric conductors, the formulation must include the scattering from the inner cylinder and the cross-coupling between the two structures. Furthermore, if one desires to design a cylindrical structure that will not permit significant propagation of electromagnetic waves interior to the structure, consideration of waveguide modes alone is not sufficient. Significant TEM modes can exist when an inner cylinder is part of the scattering problem.

The Air Force Weapons Laboratory's objective to predict scattering from structures much more complicated than the geometry considered in this thesis leads one to suggest a series of research projects related to this work. A suggestion for further study is to simulate end caps on the cylinders and various shaped apertures in the side of the outer cylinder. One could further extend the analysis by placing a cavity or enclosure behind the aperture with the inner cylinder passing through the cavity. This analysis could be further extended to include multiple apertures, cavities, and inner conductors. Finally, non-symmetrical scatterers should be analyzed. This line of research would lead to a much more accurate prediction of the scattering effects associated with complex structures.

Bibliography

1. Arsac, J. Fourier Transforms and the Theory of Distributions. Englewood Cliffs, N.J.: Prentice-Hall. Inc., 1966.

2. Collin, R.E. Field Theory of Guided Waves. New York: McGraw-Hill, 1960.

3. Davis, W.A. "A Guide to Choosing Basis and Testing Functions in the Method of Moments", presented at the USNC/URSI Meeting at the University of Illinois at Urbana-Champaign. (June 1975)

4. Davis, W.A. Numerical Solutions to the Problems of Electromagnetic Radiation and Scattering by a Finite Hollow Cylinder, Ph.D. Dissertation, University of Illinois at Urbana-Champaign, 1974.

5. Dwight, H.B. Tables of Integrals and Other Mathematical Data (Fourth Edition). New York: The Macmillan Co., 1961.

6. Harrington, R.F. Field Computation by Moment Methods. New York: The Macmillan Co., 1968.

7. Harrington, R.F. Time Harmonic Electromagnetic Fields. New York: McGraw-Hill, 1964.

8. Jordan, E.C., and K.G. Balmain. Electromagnetic Waves and Radiating Systems. Englewood Cliffs, N.J.: Prentice-Hall, Inc., 1968.

9. Papas, C.H. Theory of Electromagnetic Propagation. New York: McGraw-Hill, 1965.

10. Pierce, B.O. Elements of the Theory of the Newtonian Potential Function. New York: Ginn and Co., 1886.

11. Unz, H. "Scalar-Vector Analog of Green's Theorem." IRE Transactions on Antennas and Propagation, 6:300 (July 1958)

12. Wylie, C.R. Advanced Engineering Mathematics. New York: McGraw-Hill, 1975.

Appendix

Two identies were used in Chapter II which enables one to write the curl and the gradient of the divergence of the magnetic vector potential $\bar{A}(\bar{r})$ in a convenient form. This appendix demonstrates the validity of these identities. The restriction placed on the identities was that the observation point was not on the surface of the scatterer, $\bar{r} \neq \bar{r}'$.

Consider Eq (28)

$$\nabla \times \oint_S \nabla' \Phi \times (\hat{n}' \times \bar{A})\, ds' = -\oint_S \Phi\, \hat{n}' \times k^2 \bar{A}\, ds' - \nabla\left(\nabla \cdot \oint_S \Phi\, \hat{n}' \times \bar{A}\, ds'\right) \tag{28}$$

Interchanging the order of integration and differentiation the left side of Eq (28) in accordance with Leibnitz's rule (Ref 12:313) yields

$$\oint_S \nabla \times \left[\nabla' \Phi \times (\hat{n}' \times \bar{A})\right] ds' \tag{127}$$

which may be rewritten as

$$\oint_S \Big\{ \left[(\hat{n}' \times \bar{A}) \cdot \nabla\right] \nabla' \Phi - (\nabla' \Phi \cdot \nabla)(\hat{n}' \cdot \bar{A}) - (\hat{n}' \times \bar{A})(\nabla \cdot \nabla' \Phi) + \nabla' \Phi \left[\nabla \cdot (\hat{n}' \times \bar{A})\right] \Big\}\, ds' \tag{128}$$

Note that

$$\nabla(\hat{n}' \cdot \bar{A}) = 0 \tag{129}$$

and

$$\nabla \cdot (\hat{n}' \cdot \bar{A}) = 0 \tag{130}$$

since $(\hat{n}' \times \bar{A})$ and $(\hat{n}' \cdot \bar{A})$ are functions of the prime coordinates only. Therefore, Eq (28) simplifies to

$$-\oint_S \Phi\, \hat{n}' \times k^2 \bar{A}\, ds' + \oint_S \left[(\hat{n}' \times \bar{A}) \cdot \nabla\right] \nabla' \Phi =$$

$$-\oint_S \Phi\, \hat{n}' \times k^2 \bar{A}\, ds' - \nabla\left(\nabla \cdot \oint_S \Phi\, \hat{n}' \times \bar{A}\, ds'\right) \tag{131}$$

where Eq (26) implies $\nabla \cdot \nabla' \Phi = k^2 \Phi$ for $\bar{r} \neq \bar{r}'$ and $\nabla \Phi = -\nabla' \Phi$.

Consider the expression

$$-\nabla\left(\nabla \cdot \oint_S \Phi\, \hat{n}' \times \bar{A}\, ds'\right) \tag{132}$$

which may be written as

$$-\nabla \oint_S \left[(\hat{n}' \times \bar{A}) \cdot \nabla \Phi + \Phi\, \nabla \cdot (\hat{n}' \times \bar{A})\right] ds' \tag{133}$$

after interchanging the integration and divergence operators or

$$-\nabla \oint_S (\hat{n}' \times \bar{A}) \cdot \nabla \Phi \, ds' \tag{134}$$

since $\nabla \cdot (\hat{n}' \times \bar{A})$ is zero by Eq (130). Interchanging the order of integration and differentiation in Eq (133) permits one to write the expression as

$$-\oint_S \left\{ (\nabla \Phi \cdot \nabla)(\hat{n}' \times \bar{A}) + \left[(\hat{n}' \times \bar{A}) \cdot \nabla \right] \nabla \Phi \right\} ds' \tag{135}$$

Using Eq (129) one can write Eq (134) as

$$\oint_S \left[(\hat{n}' \times \bar{A}) \cdot \nabla \right] \nabla' \Phi \, ds' \tag{136}$$

which completes the proof.

The second identity used was

$$\nabla \left[\nabla \cdot \oint_S \hat{n}' \Phi \times \nabla' (\nabla' \cdot \bar{A}) \, ds' \right] = 0 \tag{29}$$

which may be rewritten as (Ref 7:450)

$$\nabla \left[\nabla \cdot \int_V \nabla' \times \Phi \, \nabla' (\nabla' \cdot \bar{A}) \, dv' \right] = 0 \tag{137}$$

Expanding the left side of Eq (138) yields

$$\nabla\left\{\nabla\cdot\int_V\left[\nabla'\Phi\times\nabla'(\nabla'\cdot\bar{A})+\Phi\,\nabla'\times\nabla'(\nabla'\cdot\bar{A})\right]dv'\right\}=0 \tag{138}$$

or

$$\nabla\left\{\nabla\cdot\int_V\nabla'\Phi\times\nabla'(\nabla'\cdot\bar{A})\,dv'\right\}=0 \tag{139}$$

since the curl of a gradient is equal to zero.

Interchanging the divergence and integration operators on the left side of Eq (140) and expanding yields

$$\nabla\int_V\left\{\nabla'(\nabla'\cdot\bar{A})\cdot(\nabla\times\nabla'\Phi)-\nabla'\Phi\cdot\left[\nabla\times\nabla'(\nabla'\cdot\bar{A})\right]\right\}dv'=0 \tag{140}$$

which is indeed equal to zero since the curl of a gradient is equal to zero.

VITA

David Grayson Ardis was born on 20 March 1945 in Charlottesville, Virginia. He graduated from high school in Athens, Tennessee in 1963 and attended the United States Air Force Academy from which he received the degree of Bachelor of Science in Engineering Sciences and a commission in the United States Air Force in June 1967. He completed navigator training and received his wings in September 1968. He completed electronic warfare officer training and served as an electronic warfare officer in B-52s with the 320th Heavy Bombardment Wing, Mather Air Force Base, California and in EB-66s with the 42nd Tactical Electronic Warfare Squadron, Korat Royal Thai Air Force Base, Thailand. He then served as an instructor with the 453rd Flying Training Squadron, Mather Air Force Base, California. Prior to entering the Air Force Institute of Technology, he was serving as a curriculum manager for the 323rd Flying Training Wing, Mather Air Force Base, California.

Permanent address: Box 81
Englewood, Tennessee 37329

UNCLASSIFIED

SECURITY CLASSIFICATION OF THIS PAGE (When Data Entered)

REPORT DOCUMENTATION PAGE		READ INSTRUCTIONS BEFORE COMPLETING FORM
1. ~~REPORT NUMBER~~ (14) GE/EE/76-[redacted]13	2. GOVT ACCESSION NO.	3. RECIPIENT'S CATALOG NUMBER
4. TITLE (and Subtitle) (6) ELECTROMAGNETIC SCATTERING BY CONCENTRIC FINITE CYLINDERS.		5. TYPE OF REPORT & PERIOD COVERED MS Thesis
		6. PERFORMING ORG. REPORT NUMBER
7. AUTHOR(s) (10) David G. Ardis (GRAYSON) Captain, USAF		8. CONTRACT OR GRANT NUMBER(s) (9) master's thesis,
9. PERFORMING ORGANIZATION NAME AND ADDRESS Air Force Institute of Technology(AFIT-EN) Wright-Patterson AFB, Ohio 45433		10. PROGRAM ELEMENT, PROJECT, TASK AREA & WORK UNIT NUMBERS
11. CONTROLLING OFFICE NAME AND ADDRESS Air Force Weapons Laboratory (ELP) Air Force Systems Command Kirtland Air Force Base, NM 87117 (11)		12. ~~REPORT DATE~~ Dec[redacted] 1976
		13. NUMBER OF PAGES 67 (12) 70p.
14. MONITORING AGENCY NAME & ADDRESS(if different from Controlling Office)		15. SECURITY CLASS. (of this report) Unclassified
		15a. DECLASSIFICATION/DOWNGRADING SCHEDULE

16. DISTRIBUTION STATEMENT (of this Report)

Approved for public release; distribution unlimited

17. DISTRIBUTION STATEMENT (of the abstract entered in Block 20, if different from Report)

18. SUPPLEMENTARY NOTES

Approved for public release; IAW AFR 190-17

Jerral F. Guess

JERRAL F. GUESS, Captain, USAF
Director of Information

19. KEY WORDS (Continue on reverse side if necessary and identify by block number)

Electromagnetic Scattering
EMP Coupling
EMP Interaction
Numerical Techniques in EM
Scattering by Concentric Finite Cylinders

20. ABSTRACT (Continue on reverse side if necessary and identify by block number)

This thesis deals with electromagnetic scattering from two concentric finite length cylinders. The scattering bodies are assumed ~~to be perfect~~ electric conductors and the incident field is assumed to be a plane wave whose magnetic field is transverse to the longitudinal axis of the scatterers. Electromagnetic field equations are derived in terms of vector potentials. Integral equations are developed for the surface currents induced on the cylinders. A numerical solution is → next page

DD FORM 1 JAN 73 1473 EDITION OF 1 NOV 65 IS OBSOLETE

012225 UNCLASSIFIED

SECURITY CLASSIFICATION OF THIS PAGE (When Data Entered) formulated in terms of the method of moments for the unknown surface currents and the components of the scattered electric field. Results are presented for scatterers of different dimensions. Comparisons are made between scattering from a finite hollow cylinder and scattering from two concentric finite cylinders.